Astronomy
&
Astrophysics

Long-term starspot evolution, activity cycle and orbital period variation of RT Lacertae

A. F. Lanza[1], S. Catalano[1], M. Rodonò[1,2], C. İbanoğlu[3], S. Evren[3], G. Taş[3], Ö. Çakırlı[3], and A. Devlen[3]

[1] Osservatorio Astrofisico di Catania of the Istituto Nazionale di Astrofisica, Italy
   e-mail: scatalano, mrodono@ct.astro.it

[2] Dipartimento di Fisica e Astronomia dell'Università degli Studi di Catania, Via S. Sofia, 78 – 95123 Catania, Italy,

[3] Ege University Observatory, Bornova, İzmir, Turkey
   e-mail: ibanoglu, evren, tas, cakirli@astronomy.sci.ege.edu.tr

Abstract. A sequence of V-band light curves of the active close binary RT Lacertae (G5+G9 IV), extending from 1965 to 2000, is presented and analysed to derive the spot distribution and evolution on the component stars. In our modelling approach, the Roche geometry and Kurucz's atmospheric models were adopted. The resulting maps of the spot surface distribution were regularized by means of the Maximum Entropy and Tikhonov criteria to take full advantage of the increased geometrical resolution during eclipses. By comparing the maps obtained with these two criteria, it was possible to discriminate between surface features actually required by the data and artifacts introduced by the regularization process. Satisfactory fits were obtained assuming spots on both components and the unspotted V-band luminosity ratio: $L_{G5}/L_{G9\,IV} = 0.65 \pm 0.05$. The more massive G5 primary appears to be the most active star in the system and its spotted areas are mainly responsible for the light curve distortions. The yearly spot distributions on both components indicate that their spot patterns consist of two components, one uniformly and the other non-uniformly distributed in longitude, the latter suggesting the presence of preferential longitudes. In particular, spots are concentrated around the substellar points and their antipodes on both stars. The eclipse scanning reveals spots with diameters of $\sim 40°$, or possibly smaller, on the hemisphere of the primary star being occulted. The primary shows clear evidence for a short-term activity cycle with a period of ~ 8.5 yr and a possible long-term cycle with a period of approximately 35 yr. The variation of the spot migration rate may be related with surface differential rotation, with a lower limit of $\Delta\Omega/\Omega \sim 3.2 \times 10^{-3}$. The G9 IV secondary does not show evidence for an activity cycle, its spot coverage appearing rather constant at $\sim 15-20\%$ of its surface. The relative amplitude of its surface differential rotation, as indicated by the variation of the spot migration rate, is $\Delta\Omega/\Omega \sim 2.7 \times 10^{-3}$. The variation of the orbital period shows a correlation with the activity level of the primary component. Specifically, the decreases of the orbital period appear to be associated with minimum spottedness and sizeable changes of the surface spot distribution that may be related to increases of the rotation rate of the spot pattern. Conversely, an episode of increase of the orbital period was related to an increase of the spotted area on the primary star. Such results support the recently proposed models that connect the perturbations of the orbital dynamics with the variation of the figure of equilibrium of the active components, due to the operation of non-linear hydromagnetic dynamos in their extended convective envelopes.

Key words. stars: activity – binaries: close – binaries: eclipsing – stars: individual: RT Lacertae – starspots

1. Introduction

RT Lacertae (HD 209318, SAO 51563, BD +43° 4112) is a chromospherically active close binary whose components show strong Hα and Ca II H&K emission (Huenemoerder & Barden 1986; Popper 1991; Frasca & Catalano 1994) and radio and X-ray emission from their coronae which are signatures of intense magnetic activity (Gibson et al. 1978; Umana et al. 1993; Dempsey et al. 1993). The sys-

tem is a double-lined eclipsing binary and it was initially classified by Hall (1976) as a member of the RS Canum Venaticorum group. A great deal of photometric data is available starting from the first visual and photographic observations collected at the end of the XIX century. The photometric observations prior to 1970 were studied by Haslag (1977) and the main results were summarized by Hall & Haslag (1976) and Eaton & Hall (1979). The light curves of RT Lac show a wave-like distortion outside eclipse whose amplitude and phase change with time, as typically observed in RS CVn binaries. Moreover, the

duration of the eclipses and the ellipticity coefficients were reported to be variable by Haslag (1977) and Eaton & Hall (1979). However, their conclusions are mainly based on old visual and photographic light curves, the accuracy of which is rather low. Photoelectric photometry showed another striking peculiarity of RT Lac, that is the system at mid primary eclipse was bluer than at the secondary eclipse, contrary to the situation observed in RS CVns and Algols, in which a system at the center of the deeper eclipse has a redder color because the later type component is in view.

The first attempts at modelling RT Lac light curves ascribed the distortion wave and the peculiarity of the color index to the presence of an inhomogeneous scattering envelope around the more massive component. It was assumed to be maintained by the mass transfer from the other component, which almost completely fills its Roche lobe (Milone 1976; Haslag 1977). Moreover, Eaton & Hall (1979) suggested that the apparent changes in eclipse duration and ellipticity might be due to a variation of the radius of the Roche lobe filling component. The spectroscopic studies by Huenemoerder (1985, 1988) and Huenemoerder & Barden (1986) provided clear evidence of excess emission and absorption in the Hα line, with remarkable time variability. This was interpreted as evidence for strong chromospheric activity, as well as mass loss from the less massive lobe-filling star.

The spectroscopic and photometric investigation by Popper (1991) did provide a more detailed picture of the system. The cooler component dominated the spectrum of the system, except when it was eclipsed, making it difficult to characterize the spectrum of the hotter component. Popper (1991) classified the spectral types as approximately G5 for the hotter and G9 IV for the cooler lobe-filling component. The hotter component was found smaller and more massive than its companion and well detached from its Roche lobe. Popper (1991) attributed the distortion wave and the other photometric peculiarities to the presence of cool spots on the hotter component. These spots cover a large fraction of the photosphere ($\approx 30-50\%$) making the mean surface brightness of the star lower than that of the cooler component. Therefore, the deeper eclipse occurs when the hotter and heavily spotted star is in front, which explains the bluer color at that phase being the color index dominated by its unspotted photosphere. The contribution from the occulted cooler component is very small at mid eclipse because the fractionary radii of the two components are quite similar.

Although RT Lac shares with the RS CVn binaries most of their basic characteristics, in particular the spectroscopic and photometric peculiarities associated with strong magnetic activity, it differs from the classical RS CVn's because it is a semi-detached binary with the secondary component almost completely filling its Roche lobe. Moreover, the mass ratio is remarkably different from unity, which suggests that the evolution of the lobe-filling and less massive component had been significantly affected by mass loss. Actually, Milone (1976, 1977) suggested that

the photometric peculiarities of RT Lac could be associated with mass transfer or mass loss processes rather than magnetic activity.

Popper (1991) described some of the characteristics of the group of chromospherically active binaries with mass ratio far from unity, suggesting that the observed phenomenology is more likely due to magnetic related activity in their atmospheres, rather than being associated with mass loss or mass transfer. Hall (1989) regarded RT Lac as a system at the boundary between RS CVn and classical Algols with a late-type secondary, characterized by strong magnetic activity supported by a powerful dynamo action in rapidly rotating deep convection zones.

In the present investigation we shall study the long-term photometry of RT Lac and model the variations of its light curves in the framework of the starspot hypothesis. Our aim is to study the main characteristics of the photospheric activity on each component by adopting the same approach we have already used to model other classical RS CVn binaries, notably the prototype itself (Rodonò et al. 1995), AR Lac (Lanza et al. 1998a), II Peg (Rodonò et al. 2000) and SZ Psc (Lanza et al. 2001). It assumes that the photospheres of both components are covered by small solar-sized spots with a temperature lower than the surrounding photosphere. Their surface distribution is iteratively adjusted in order to fit the observed light curves. The simultaneous fitting of a long-term sequence of light curves with the same set of geometric and photometric parameters allows us to remove most of the ambiguities of the spot modelling approach and yields an accurate determination of the variation of the total spotted area versus time. In this way, it is possible to detect activity cycles in the components. Moreover, the longitude distributions of the spotted area in different years can be compared to search for active longitudes and investigate their complex phenomenology (cf. Lanza et al. 1998a; Rodonò et al. 2000). Starspots may also be used as rotation tracers to investigate the surface differential rotation and the spin-orbit synchronization.

An interesting peculiarity of RT Lac is its variable orbital period, the changes of which were derived from long-term eclipse timing. The modulation of the orbital period is indeed a peculiar characteristic of magnetically active close binaries (cf. Hall 1989) and several models have been proposed to link the operation of the stellar hydromagnetic dynamos with the perturbations of the orbital dynamics (Applegate 1992; Lanza et al. 1998b). The phenomenological connection between orbital period changes and magnetic activity in RS CVn and Algol binaries needs further investigation and RT Lac is one of the most suitable systems, as demonstrated by Keskin et al. (1994) and İbanoğlu et al. (2001). The possibility of correlating the variation of the activity level and of the rotation regime, as derived from light curve spot modelling, with the orbital period changes offers a unique opportunity to investigate the energy balance of non-linear hydromagnetic dynamos in stars and the system dynamics, as discussed by Lanza & Rodonò (1999).

2. Observations

Our data set consists of twenty-six yearly light curves of RT Lac obtained from 1965 to 2000. The 1965–68 data are from Hall and Milone and were described in detail by Milone (1977). The 1977 light curve was retrieved from the archive of unpublished observations of Catania Astrophysical Observatory. The other light curves were obtained at Ege University Observatory, where a monitoring program of RT Lac has been carried out since 1978.

In the present analysis we consider only the V-band light curves of RT Lac because they are the most complete and homogeneous. All our magnitudes are referred to BD +43°4108 (HD 209219, SAO 51542), the comparison star adopted by almost all the observers because it is close to the variable and have similar colors, making negligible the correction for differential atmospheric extinction. BD +43°4109 (HD 209220, SAO 51544) was usually adopted as a check star.

In addition to the listed light curves, there were also some sparse photometric observations collected in 1972 by Milone (cf. Milone 1976) which were not considered in the present study because of their poor phase coverage.

The orbital period being very close to five days, it is difficult to obtain a good phase coverage of the light curve from a single observing site in a short time interval. Therefore, although some points appear close in phase, they could have been obtained after an interval of several weeks or a few months, during which the system may have undergone significant variations. Indeed, RT Lac is a very active system and out-of-eclipse light variations up to 0.03–0.05 mag have been observed during the course of the same night. Due to the system's intrinsic variability and the unfavourable orbital period, some light curves show phase gaps and large data dispersion with intrinsic standard deviations up to $\sim 0.03-0.05$ mag. In order to avoid a loss of information by averaging such variations, for the analysis the observations were not averaged into normal points, except in the case of the 1965 and 1968 light curves, for which only the normal points listed by Milone (1977) were available to us. All light curve data points were given the same weight, as done by Lanza et al. (1998a).

An important issue concerns the specification of the ephemerides adopted to put the observations in phase. The deeper minimum in the light curve was identified by the first observers as the primary minimum, according to the usual definition adopted for eclipsing binaries, and its orbital phase was assumed to be 0.0 (cf. Haslag 1977). However, such an assumption turned out to be unsatisfactory for RT Lac because the magnitude at the center of the so-defined primary minimum showed large time variations, with the system sometimes being brighter than at the secondary minimum, and the color index was bluer than that of the secondary minimum, in clear disagreement with the observations of other close active binaries. The recent studies by Popper (1991) and İbanoğlu et al. (2001) clarified the cause of this unusual behaviour and

pointed out that the choice of the primary minimum was not appropriate. They found that RT Lac is peculiar because its primary is so heavily spotted that the deeper minimum in most light curves turned out to be that with the primary in front, despite its earlier spectral type. A consequence of the spot activity is also that the magnitude at the center of the primary minimum changes remarkably in time because of the large variation of the spotted area on the primary star. Conversely, the magnitude at the center of the secondary minimum appears to be more stable (cf. Ibanoglu et al. 2001). In view of such considerations, it seemed to us more appropriate to define as the primary minimum that when the more massive and hotter component is eclipsed by the less massive and cooler component, according to the normal assumption made for RS CVn and other binaries. An advantage of this choice is that the color index of the system at the primary minimum is redder than at the secondary, as in the other binaries.

In order to make easier the transition to the new definition of the epochs of primary minima, we shall list the epochs of the primary minima as given in the original literature references as well as those revised according to the present assumption by adding a half orbital period to the epochs specified by the old ephemerides. Specifically in Table 1 we give for each light curve the mid epoch of the observations, the time span of the observations (ΔT), the number of normal points (M), the aperture of the telescope used (D_{T}), the photometric system (S means standard UBV), the primary minimum of the ephemeris used in the literature and the revised primary minimum adopted in the present study, the period of the ephemeris and the literature reference.

The overall variation of the system's magnitude versus time is plotted in Fig. 1. In order to better display the long-term variations due to spot activity, only photometric points outside eclipses are plotted.

The brightest magnitude in our light curve sequence turns out to be $m_V = 8.642 \pm 0.006$ at orbital phase 0.7391 in the 1979 light curve. This value is assumed as the magnitude of the unspotted system, thus establishing the magnitude scale calibration for the subsequent light curve modelling.

3. Spot modelling technique

The reconstruction of the intensity distribution over the surface of a star using photometric data alone is an ill-posed problem. The wide-band flux modulation provides us with information only on the variation of the projected spot area versus phase, i.e., the stellar longitude. Some additional information on the latitudinal distribution can be extracted during eclipses, when the spot pattern on the component being occulted is scanned by the advancing disk of the other component. Nevertheless, the problem remains ill-posed even in the most favourable conditions.

We notice that one can select a unique spot distribution by minimizing the χ^2 of the residuals between the

Table 1. V-band light curves of RT Lac.

Light curve	Mid Epoch (HJD − 2400000)	ΔT (d)	M	D_T (cm)	P	Primary Minimum Epochs (HJD-2400000) (a)	(b)	Period (days)	Reference
1965	39053.6	37	59	41–91	S	40382.8910	40385.4280	5.0740150	Milone (1977)
1968	40203.9	90	51	44–138	S	40382.8910	40385.4280	5.0740150	Milone (1977)
1977	43362.5	38	66	91	S	43772.3165	43774.8535	5.0740010	present paper
1978	43734.4	95	169	48	S	43772.3165	43774.8535	5.0740010	İbanoğlu et al. (1980)
1979	44105.4	172	194	48	S	43772.3165	43774.8535	5.0740010	İbanoğlu et al. (1980)
1980	44468.3	68	369	48	S	43772.3165	43774.8535	5.0740010	Tunca et al. (1983)
1981	44878.2	110	386	48	S	43772.3165	43774.8535	5.0740010	Tunca et al. (1983)
1982	45237.9	149	281	48	S	45162.5771	45165.1141	5.0739900	Evren et al. (1985)
1983	45582.4	94	202	48	S	45532.9792	45535.5162	5.0739900	Evren et al. (1985)
1984	45914.4	110	357	48	S	45857.7029	45860.2399	5.0739900	Evren (1989)
1985	46290.9	151	509	48	S	46212.8746	46215.4116	5.0739900	Evren (1989)
1986	46635.0	59	180	48	S	46603.5605	46606.0975	5.0739900	Evren (1989)
1987	47061.8	125	192	48	S	46994.2333	46996.7703	5.0739900	Evren (1989)
1988	47402.4	102	378	48	S	47349.4248	47351.9618	5.0739900	Evren (1989)
1989	47742.3	62	434	48	S	47709.6650	47712.2020	5.0739900	İbanoğlu et al. (1998a)
1990	48114.9	149	698	48	S	48039.4703	48042.0073	5.0739900	İbanoğlu et al. (1998a)
1991	48492.4	104	863	48	S	48435.2333	48437.7703	5.0739900	İbanoğlu et al. (1998a)
1992	48846.4	164	512	48	S	48759.9588	48762.4958	5.0739900	İbanoğlu et al. (1998a)
1993	49204.9	151	725	48	S	49125.2838	49127.8208	5.0739900	İbanoğlu et al. (2001)
1994	49568.9	37	136	48	S	49546.4071	49548.9440	5.0739900	İbanoğlu et al. (2001)
1995	49959.9	71	227	48	S	49921.8894	49924.4264	5.0739900	İbanoğlu et al. (2001)
1996	50292.4	64	384	48	S	50256.7689	50259.3059	5.0739900	İbanoğlu et al. (2001)
1997	50695.4	124	395	48	S	50302.4343	50304.9713	5.0739900	İbanoğlu et al. (2001)
1998	51059.8	155	609	48	S	50982.3554	50984.8924	5.0739900	İbanoğlu et al. (2001)
1999	51423.9	117	859	48	S	51362.8920	51365.4290	5.0739900	İbanoğlu et al. (2001)
2000	51804.3	132	478	48	S	51733.2839	51735.8209	5.0739900	İbanoğlu et al. (2001)

(a) Original times of primary eclipse with the more massive and variable component in front.
(b) Revised times of primary eclipse with the less massive and cooler component in front, according to the standard eclipsing binary notation.

observed and the synthetized light curve, but such an approach is unsatisfactory because the solution is unstable, i.e., small changes in the input data produce large changes in the spot map. This is due to the role played by the noise in the χ^2 minimization, which implies that most of the structures appearing in the spot map actually come from the modelling of the light fluctuations due to intrinsic variability or measurement errors.

It is possible to overcome the uniqueness and stability problems by introducing a regularizing function into the solution process. This corresponds to the a priori assumption of some specific statistical property for the spot map, which allows us to select one stable map among the potentially infinite number of maps that can fit a given light curve. The two mostly used a priori assumptions applied to the star map problem are the Maximum Entropy (hereinafter ME; Gull & Skilling 1984; Vogt et al. 1987) and the Tikhonov regularizations (hereinafter T; Piskunov et al. 1990). They are particularly suited when the spot map consists of an array which specifies the spot covering factor in each surface element (or pixel) of the model star. The covering factor f gives the specific intensity

I of each surface element according to the definition: $I = (1 - f)I_\mathrm{u} + fI_\mathrm{s}$, where I_u is the specific intensity of the unspotted photosphere of the surface element, I_s that of the spotted photosphere, and $0 < f < 1$.

A detailed description of our modelling approach, including the application of the ME and T regularizations, was presented by Lanza et al. (1998a) and we refer the reader to that paper for a detailed discussion. Here we only recall that the ME spot maps are computed by a constrained minimization of the functional:

$$Q_\mathrm{ME} = \chi^2 - \lambda_\mathrm{ME}(S_1 + S_2), \qquad (1)$$

whereas the T maps come from the constrained minimization of:

$$Q_T = \chi^2 + \lambda_\mathrm{T}(T_1 + T_2), \qquad (2)$$

where χ^2 is the normalized sum of the squared residuals between the observed and the synthetized light curves, S_k is the entropy of the spot map of the k-th star ($k = 1, 2$), T_k is the Tikhonov functional of the spot map of the k-th star and λ_ME and λ_T are the Lagrange multipliers for the Maximum Entropy and the Tikhonov regularizations,
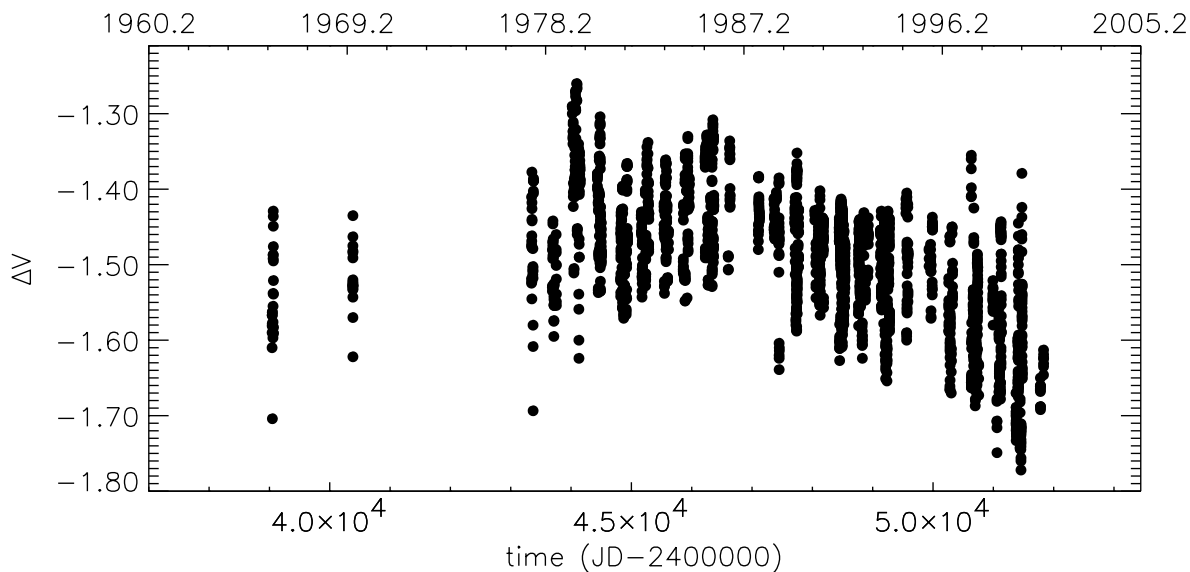
Fig. 1. The magnitude difference ΔV between the comparison HD 209219 and RT Lac versus time. Only the photometric points outside eclipses are plotted, i.e., with orbital phase ϕ in the intervals: $0.1 \leq \phi \leq 0.4$ or $0.6 \leq \phi \leq 0.9$.

respectively. The explicit expressions for χ^2, S_k and T_k and the procedure of evaluation of the Lagrange multipliers are described by Lanza et al. (1998a).

The synthetized light curve for a given distribution of the covering factor is computed using an upgraded version of the computer code introduced by Lanza et al. (1998a). The present approach adopts Roche geometry to describe the surfaces of the components. The photosphere of each component is subdivided into squared surface elements of side $s_e = 1°$ in order to warrant a relative precision of the order of $10^{-6}-10^{-5}$ in the numerical evaluation of the flux that emerges from the stellar disks. The flux from each surface element is computed by adopting Kurucz's (2000) atmospheric models with a linear limb darkening law and taking into account gravity darkening effects, according to Kopal (1959). The reflection effect is treated assuming black-body re-irradiation with a given bolometric albedo and Lambert's law for the angular distribution of the re-emitted radiation. It is interesting to note that the linear limb darkening law adopted for the angular dependence of the specific intensity allows us to work with a constant projection matrix in the light curve inversion problem and thus allows us to evaluate analytically the gradients of the objective functionals in Eqs. (1) and (2). This procedure significantly reduces the CPU time required to compute a solution (cf. Lanza et al. 1998a for details on the inversion problem). The systematic errors introduced by the linear limb darkening approximation have been reduced by computing its coefficients by means of the least square procedure proposed by Diaz-Cordoves et al. (1995) for Kurucz's models. Small errors in the atmospheric modelling give rise only to second-order effects in our analysis of stellar activity, because we are mainly interested in the differential *variation* of the spot pattern properties from season to season. Absolute properties of the spots can not be extracted from single-band data because systematic errors

arise, among others, from the unknown unspotted light levels of the system components and the assumption of single-temperature spots.

4. Model parameters

In our spot maps we adopted squared map elements of side $s = 18°$ for both components. The fluxes, however, were always computed with a finer subdivision ($s_e = 1°$). The masses and the radii of the components were taken from Popper (1991) and Eaton & Hall (1979), respectively.

The Roche lobe geometry was implemented according to Kopal (1989) with the Roche potential Ω at the surface of each star being computed from the mass ratio and the star's fractionary radius in the direction joining the centers of the two components. The fractionary radii were slightly adjusted with respect to Eaton & Hall's (1979) values to improve the fits. The values of the Roche potential and the fractionary radii at the point (i.e., along the line joining the centers of the components), side, back and pole for each component are listed in Table 2, respectively. Their accuracies are ± 0.007 and are mainly determined by the light curve fluctuations near eclipse contacts.

The effective temperature of the unspotted photosphere of the hotter primary star was estimated by Popper (1991) to be $\sim$5100 K, using the colour difference between the two components because the spectrum of the more massive primary is not so well exposed on his plates to allow a determination of its effective temperature. Eaton & Hall (1979) estimated a difference of $\sim$400 K between the effective temperatures of the two stars, hence we assume an effective temperature of 4700 K for the cooler star. The spot effective temperature was assumed to be 1000 K lower than the residual unspotted photospheres. This spot temperature is an average value for the spots on RS CVn active components, that were estimated from

Table 2. Geometrical and physical parameters adopted for modelling the RT Lac light curves.

Orbital elements of RT Lac		
Element		Ref.$(^a)$
Semi-major axis	1.00	
Eccentricity	0.00	1
Inclination (deg)	89.0	1
Time of conjunction	mid primary eclipse	
Period (day)	$\sim$5.074	1

Stellar and model parameters			
Stellar Parameter	G5:	G9 IV	Ref.$(^a)$
Roche potential (Ω)	4.170	6.326	1, 2, 3
Fract. radius (point)	0.272	0.294	1, 2, 3
Fract. radius (side)	0.268	0.263	1, 2, 3
Fract. radius (back)	0.271	0.282	1, 2, 3
Fract. radius (pole)	0.264	0.256	1, 2, 3
Mass ($M_\odot = 1$)	1.57	0.63	2
V-band fractional luminosity	0.394	0.606	3
Bolometric correction (mag)	-0.30	-0.05	4
Effective temperature (K)	5100	4700	1, 2
Surface gravity $\log g$ (cm s^{-2})	3.6	3.0	2
Starspot temperature (K)	4100	3700	3
Gravity darkening	0.25	0.25	5
u_V (unspotted)	0.764	0.793	6, 7
u_V (spotted)	0.815	0.833	6, 7
C_s	0.242	0.155	3
Bolometric albedo	1.00	0.30	5
Albedo in the V pass-band	0.99	0.26	3

$(^a)$ References: [1]: Eaton & Hall (1979); [2]: Popper (1991); [3]: present study; [4]: Allen (1973); [5]: Eaton et al. (1993); [6]: Kurucz (2000); [7]: Diaz-Cordoves et al. (1995).

modelling their infrared light curves. Unfortunately, infrared photometry of RT Lac is quite sparse (cf. Milone 1976) and was never analysed to derive spot temperatures (see, however, the discussion in Sect. 6).

Our assumption of a constant spot temperature should not induce significant errors into the geometry of the spot pattern, if the brightness of the spotted photosphere did not vary significantly from year to year. Solar observations support this assumption for the V-band, but brightness changes along the activity cycle might indeed occur in the infrared (Maltby 1992).

The latest photospheric models by Kurucz (2000) were used to evaluate the ratio of the specific intensities of the spotted and unspotted photospheres at the disk center (C_s) and the linear limb-darkening coefficients in the V-band (u_V). The adopted gravity darkening coefficients are appropriate for stars with outer convective envelopes. The bolometric albedo for the late-type G9 IV secondary was assumed smaller than unity in consideration of its extended convective envelope (cf. Eaton et al. 1993).

All model parameters we adopted to compute the light curve fits are listed in Table 2, together with the corresponding references.

Table 3. The Lagrangian multipliers and the χ^2 of the light curve fits with ME and T regularizing criteria, respectively.

Light curve	λ_{ME}	χ^2_{ME}	λ_{T}	χ^2_{T}
1965	0.5	0.679	4.0	0.677
1968	1.0	1.269	4.0	1.232
1977	2.0	7.765	90.0	8.076
1978	1.0	1.124	4.0	0.957
1979	1.5	9.444	4.0	9.290
1980	0.5	1.357	4.0	1.432
1981	1.0	0.627	40.0	0.752
1982	0.5	1.242	4.0	1.208
1983	1.5	1.934	4.0	1.543
1984	0.5	0.752	4.0	0.734
1985	0.5	0.818	4.0	0.827
1986	0.5	0.467	40.0	0.580
1987	0.5	2.014	4.0	2.092
1988	0.5	0.570	4.0	0.546
1989	0.5	0.636	4.0	0.607
1990	0.5	0.613	4.0	0.519
1991	1.0	0.806	4.0	0.680
1992	0.5	0.663	4.0	0.686
1993	0.5	1.050	4.0	1.051
1994	0.5	0.595	4.0	0.612
1995	0.5	0.324	4.0	0.301
1996	0.5	0.620	4.0	0.635
1997	0.5	1.397	4.0	1.430
1998	0.5	1.210	4.0	1.176
1999	0.5	1.183	4.0	1.180
2000	1.0	1.195	40.0	1.002

In order to fit all the light curves with constant values of the stellar fractional luminosities, at the outset we re-determined the luminosity ratio in the V-band, assuming it as an additional free parameter in the fitting procedure, as described by Rodonò et al. (1995) and Lanza et al. (1998a). By minimizing the sum of the χ^2's of the best covered light curves in the sequence, with $\lambda_{\mathrm{ME}} = 0.5$ fixed, we derived the following best value for the luminosity ratio in the V-band:

$$\frac{L_{\mathrm{hot}}}{L_{\mathrm{cool}}} = 0.65 \pm 0.05, \qquad (3)$$

where "hot" refers to the more massive primary and "cool" to the secondary component. The quoted uncertainty is an estimate of the range containing the true value of the luminosity ratio with 99% confidence level, when systematic errors are neglected (cf. Lampton et al. 1976; Rodonò et al. 2001). The above luminosity ratio led to the fractional V-band luminosities reported in Table 2.

5. Results

5.1. Light curve fitting and spot maps

The light curve fits we obtained with the model parameters listed in Table 2 and the ME criterion are shown in Figs. 2 and 3, whereas those obtained with the same parameters and the T criterion are shown in Figs. 4 and 5,
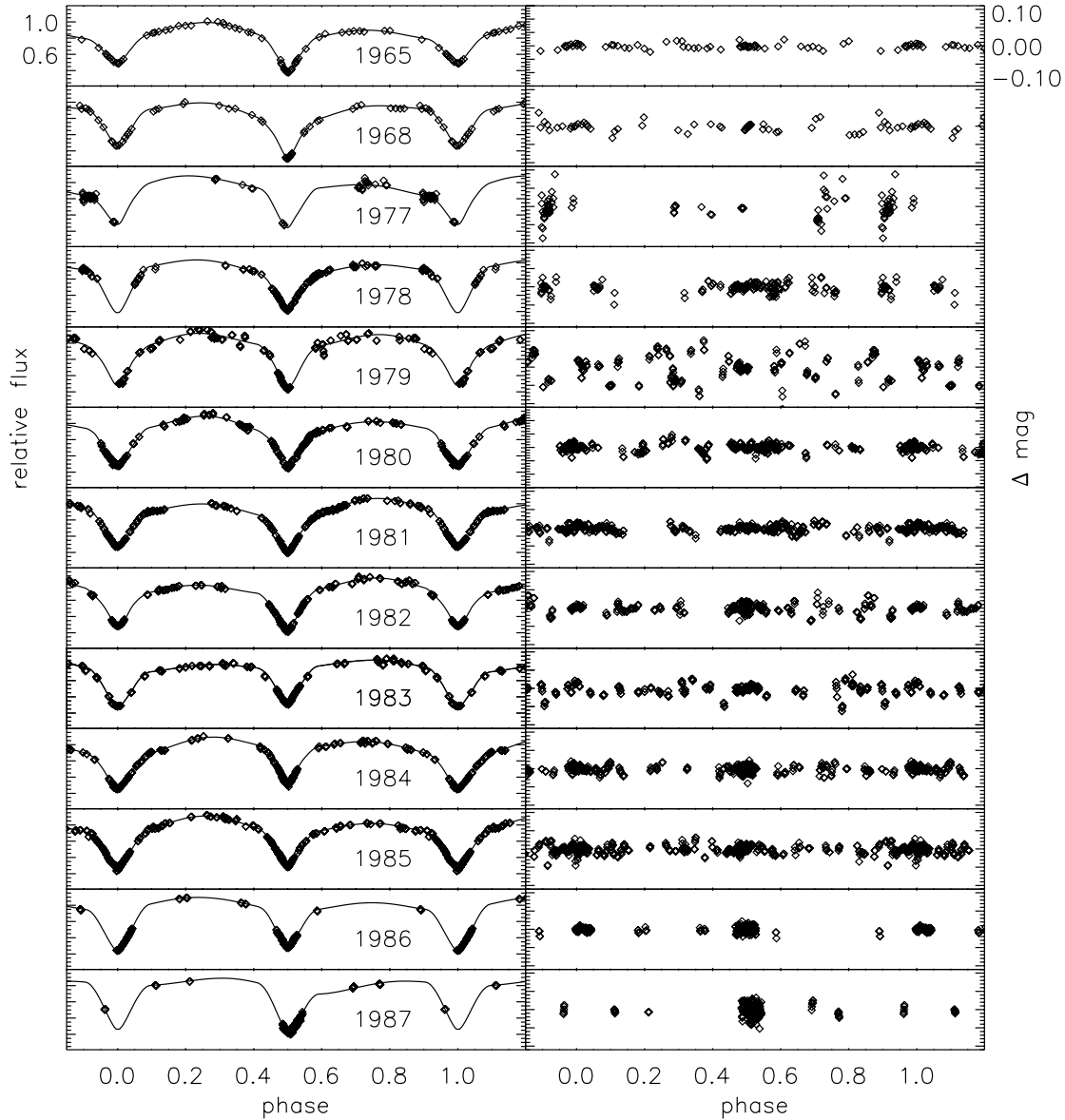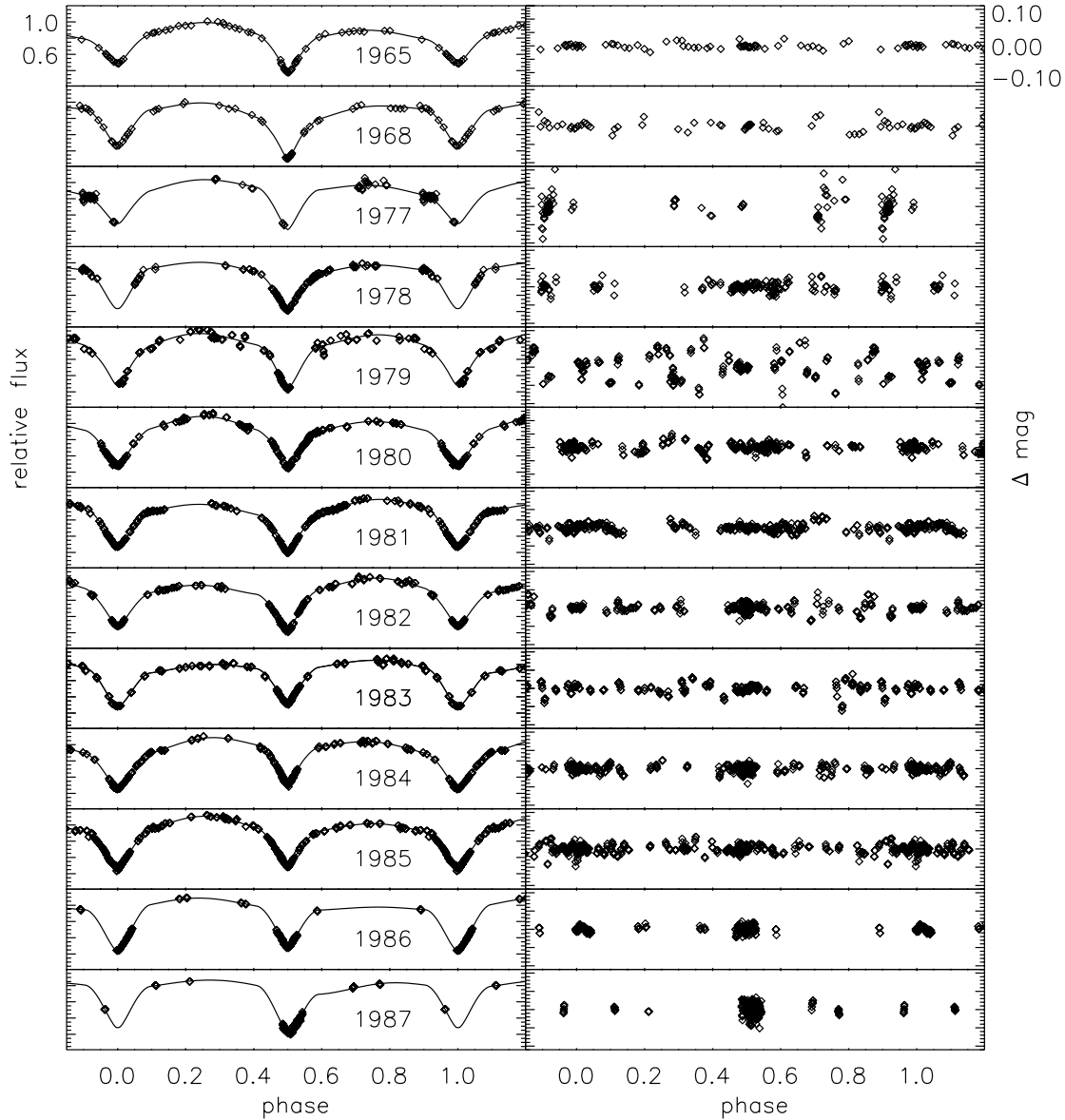
Fig. 2. The *V*-band light curve fits with the Maximum Entropy regularization criterion from 1965 to 1987 (left panels) and the corresponding residuals (right panels). Zero phase corresponds to mid primary eclipse, according to the revised ephemerides (cf. Table 1). Note that the right panel scale is about four times more expanded than the left panel scale.

respectively. The corresponding values of the Lagrange multipliers and the χ^2's are listed in Table 3. The χ^2's were computed according to Eq. (3) in Lanza et al. (1998a), assuming a standard deviation $\sigma_j = 3 \times 10^{-2}\ F_0$ for all the measurements, where F_0 is the unspotted flux of the system at quadrature. The mean standard errors of the observations turn out to be between 0.015 and 0.04 mag. Only the 1977 and 1979 light curves have a χ^2 significantly greater than unity due to the large scatter of the outside-of-eclipse data. In all cases, the fits are satisfactory and some small systematic deviations, especially during primary minima, can be accounted for by intrinsic light fluctuations of the system (see Sect. 2).

The derived distributions of the covering factor on the components are displayed using IDL and plotted on Mercator maps. Specifically, the original maps, with 18° squared pixels, were smoothed for presentation purposes to maps with a pixel side 5 times smaller, using a bi-linear interpolation (function REBIN of IDL) and then displayed as images (Figs. 6, 7, 8 and 9). On the maps of the more massive primary the longitude is measured from the substellar point in the direction opposite to the orbital motion, whereas on the secondary it is measured from the antipodes of the substellar point, again in the direction opposite to the orbital motion. Thus on all the maps the phase at which a given spot element crosses the central meridian of the stellar disk is equal to its longitude. We explicitly note that the phase is always reckoned with the revised ephemerides whose primary minima epochs are listed in Table 1.
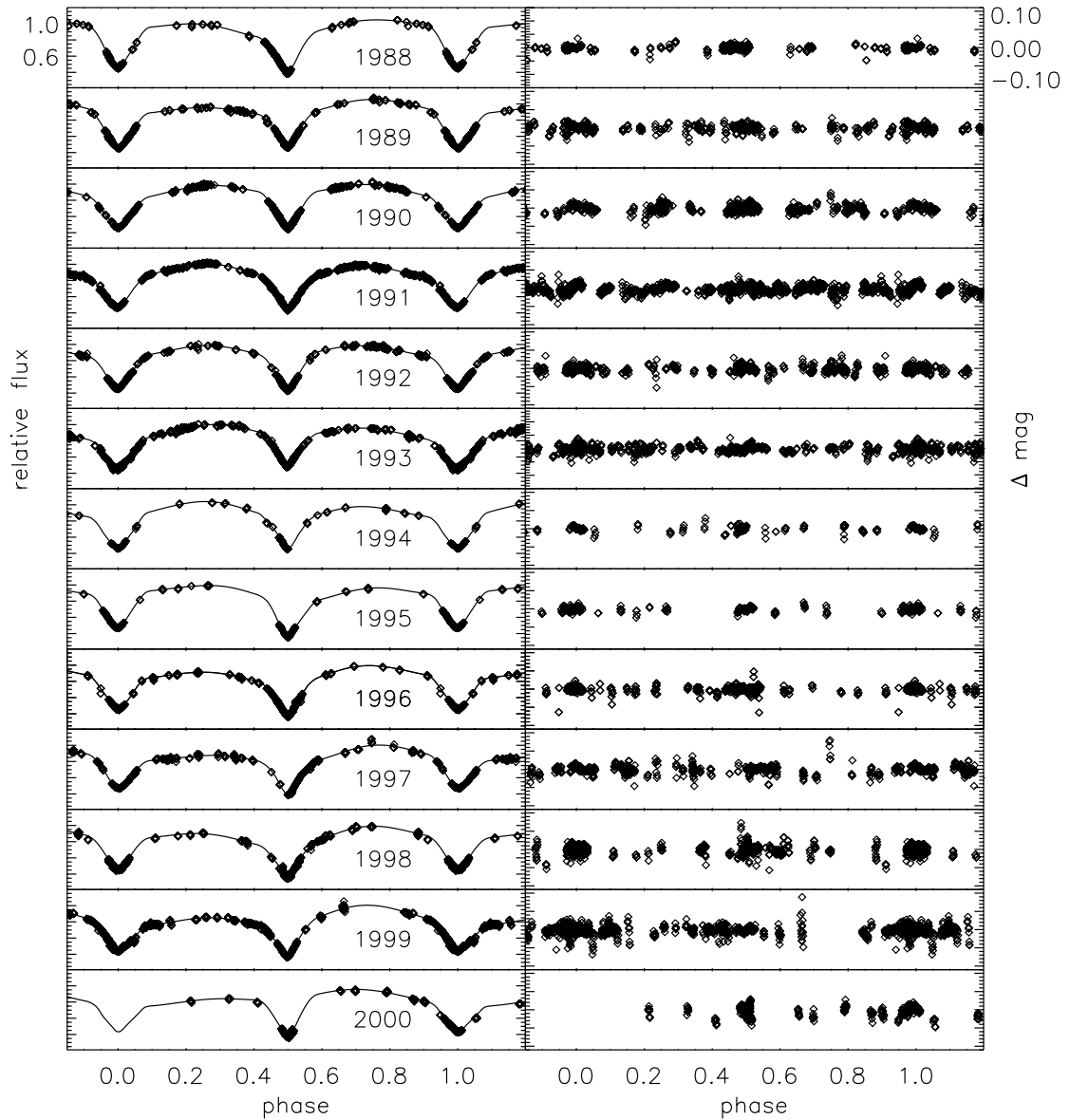
Fig. 3. As Fig. 2, but for the light curves in the time interval 1988–2000.

The ME solutions show that polar spots are not required to fit the wide-band light curves, even during eclipses when the spatial-phase resolution is increased due to the occultation of one component by the other.

Several small structures are present on the hemispheres occulted during eclipses, but they are the result of image artifacts due to the ME regularization, the so-called *super-resolution effect* (Narayan & Nityananda 1986). The actual resolution, deduced from the analysis of several simulated light curves with a pseudo-Gaussian noise of $\sigma = 0.02$ mag and $M = 40$ normal points, is $\sim 20°-30°$ on the strips occulted during eclipses and $\sim 40°-60°$ outside of them. Light curves with the same σ and a larger M have a somewhat higher resolution, but structures smaller than $30°-40°$ should in any case be regarded with caution because they are likely to be artifacts, even within the eclipsed strips.

An alternative description of the spot pattern is provided by the maps regularized with the T criterion. Those maps are the smoothest that fit the light curves. They show that several details in the ME maps are not necessarily required by the data.

The T maps of the more massive primary are quite similar to the ME maps, both showing two large spot concentrations around longitudes 0° and 180°, respectively. The activity maximum seems to switch from one longitude to the other, although since 1996 both appear to have been simultaneously active. The active longitude around 0°, i.e., near the substellar point on the hemisphere facing the companion star, has an extension of $\sim 120°-150°$ and is markedly inhomogeneous on the ME maps. The T maps confirm the presence of substructures down to the resolution limit of the eclipse mapping technique ($\sim 30°-40°$), although with a lower degree of contrast. The active

Fig. 4. The V-band light curve fits with the Tikhonov regularization from 1965 to 1987 (left panels) and the corresponding residuals (right panels). Zero phase corresponds to mid primary eclipse, according to the revised ephemerides (cf. Table 1). Note that the right panel scale is about four times more expanded than the left panel scale.

longitude centered at $180°$ is more compact and homogeneous with a longitudinal extension of $\sim60°-80°$. It is important to note that this active longitude is never occulted during eclipses, hence it is mapped with a lower resolution than the active longitude around $0°$ which is occulted at primary eclipse.

A drawback of the T regularization would be the presence of a high latitude spot pattern, which is not actually needed to fit our data, as shown by the ME fits. Photometric data give very poor constraints on the high latitude features which are dominated by the regularization. This produces an extension of some features towards the poles and a uniformly grey area at high latitudes, smoothing out the variation of the covering factor over

the star surface and increasing the total spotted area with respect to the ME maps.

The ME maps of the G9 IV secondary usually show three active longitudes, the one around longitude $180°$ is the more contrasted and persistent. On the T maps, such an active longitude is also well detected, whereas the other two are much less contrasted and difficult to identify. The active longitude around $180°$ is on the hemisphere facing the primary star and occulted at primary eclipse, thus it is mapped better than the other surface features. It is quite compact with a longitudinal extension of $\sim60°$ on the T maps.

The distributions of the spotted area vs. longitude are shown in Figs. 10 and 11 for the more massive primary component and in Figs. 12 and 13 for the G9 IV
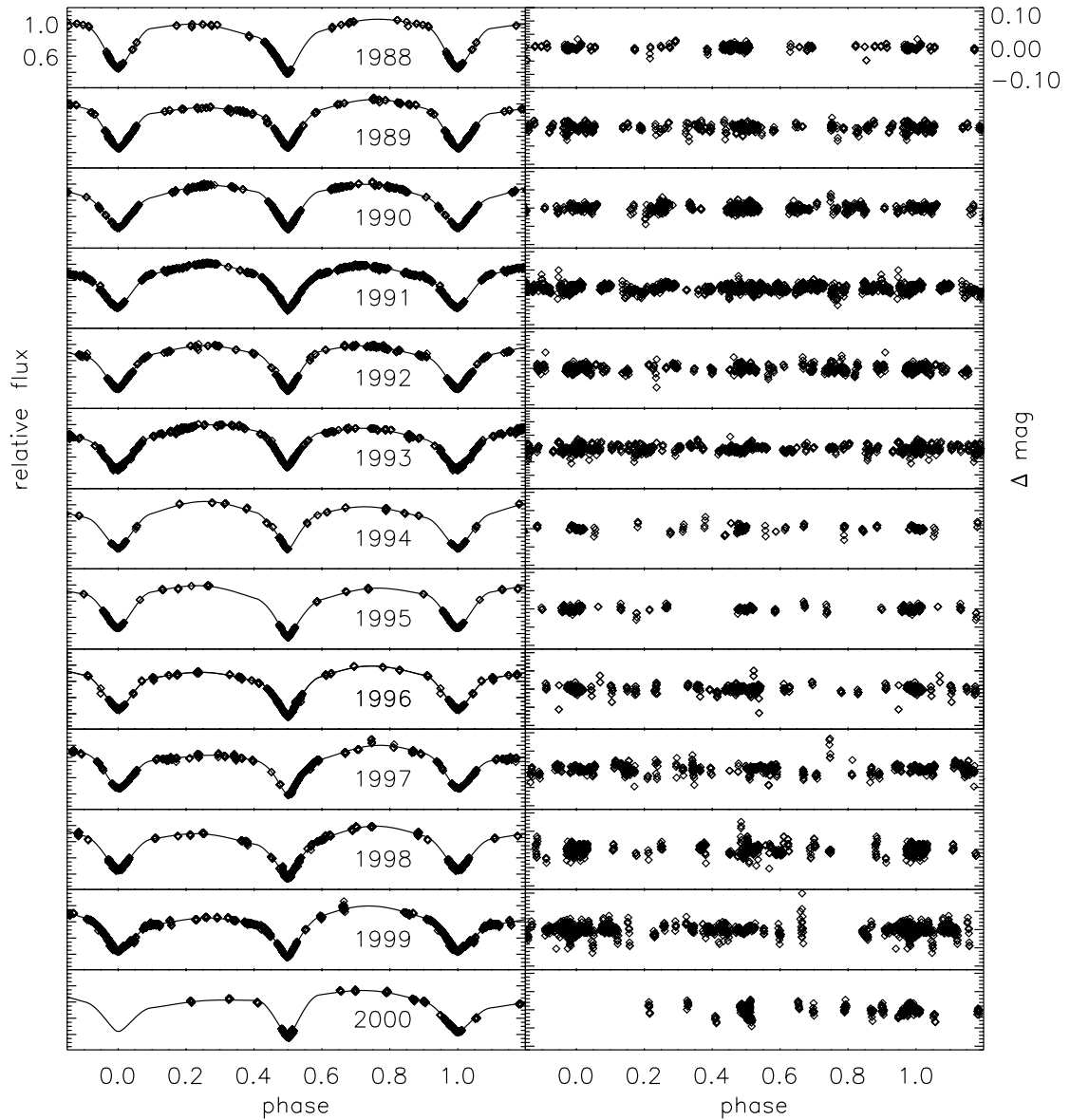
Fig. 5. As Fig. 4, but for the lightcurves in the time interval 1988–2000.

secondary component, respectively. The plotted distributions are those derived from the actual spot covering factor, binned into 18° longitude intervals, without any smoothing with the IDL REBIN function. The ME distributions give the lowest area per longitude bin actually required by the data and the assumed system parameters and unspotted magnitude. The relative uncertainties are within the dimensions of the plotting symbols (cf. Lanza et al. 1998a for more details on the accuracy of the derived spot areas).

The maps obtained with the T regularization usually show a significantly larger spotted area per longitude bin than those obtained with the ME criterion, due to the presence of the high latitude "grey caps".

Each distribution of spotted area vs. longitude can be represented as the sum of a uniform term a_U, which is defined as the minimum spotted area at all longitudes, and a term $a_D(l)$ which varies vs. longitude l. The latter term often shows more than one relative maximum and minimum, thus suggesting the presence of several preferential longitudes.

5.2. Overall evolution of the spot pattern

The total area covered by spots ($A = A_U + A_D$), and the total areas of the uniform ($A_U = \int_0^{2\pi} a_U dl$) and longitude-dependent ($A_D = \int_0^{2\pi} a_D dl$) components, are plotted vs. time in Figs. 14a, 14b and 14c for the primary component and in Figs. 15a, 15b and 15c for the G9 IV secondary component, respectively. The relative uncertainties of the values of A, that we can estimate from the solutions' stability, are ∼15%−25% for the primary component and ∼5%−10% for the more luminous secondary.

The total spotted area on the more massive primary varies from 7% to 29% in the ME models and from 12% to 49% in the T models. The ME models tend to
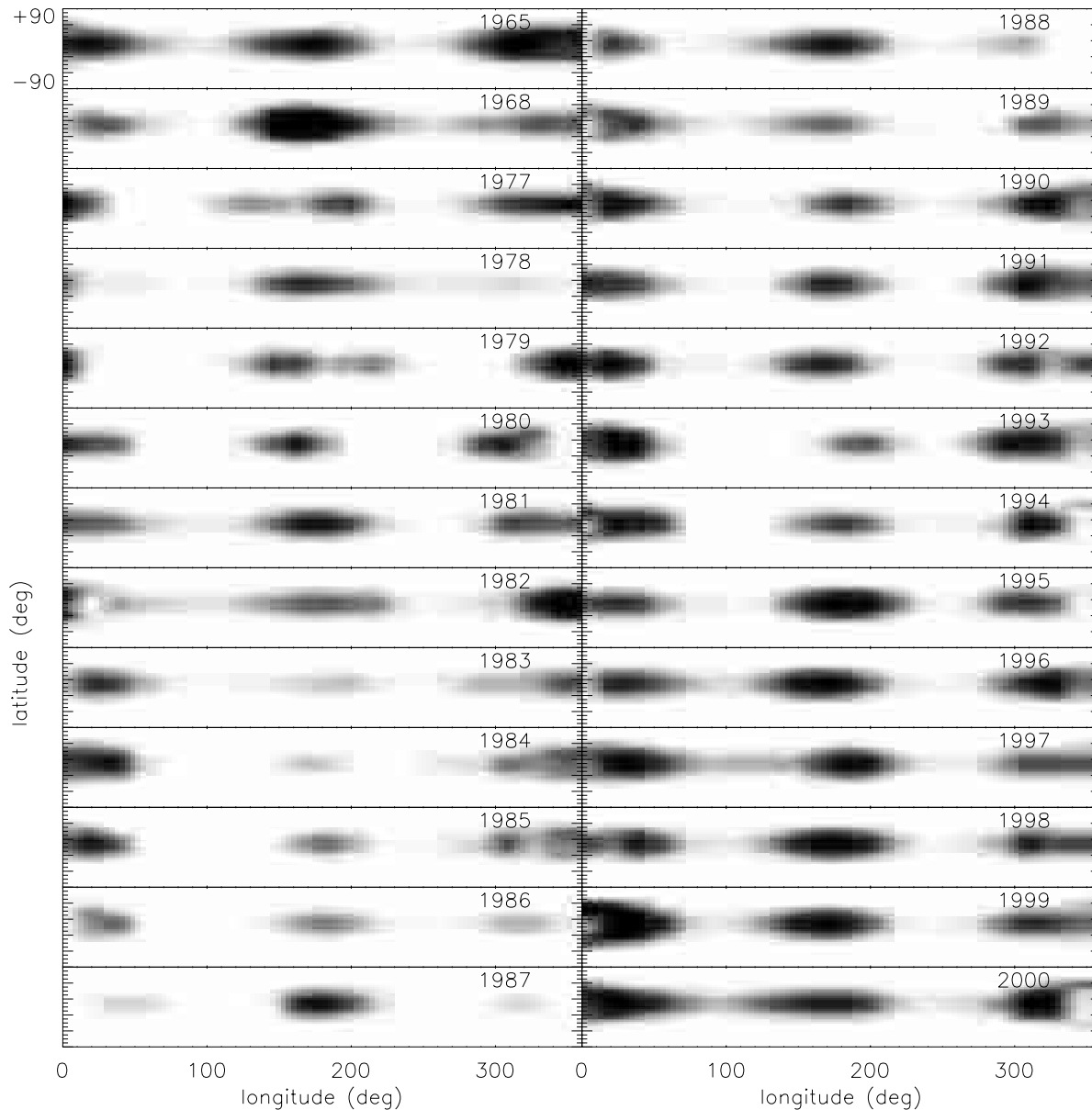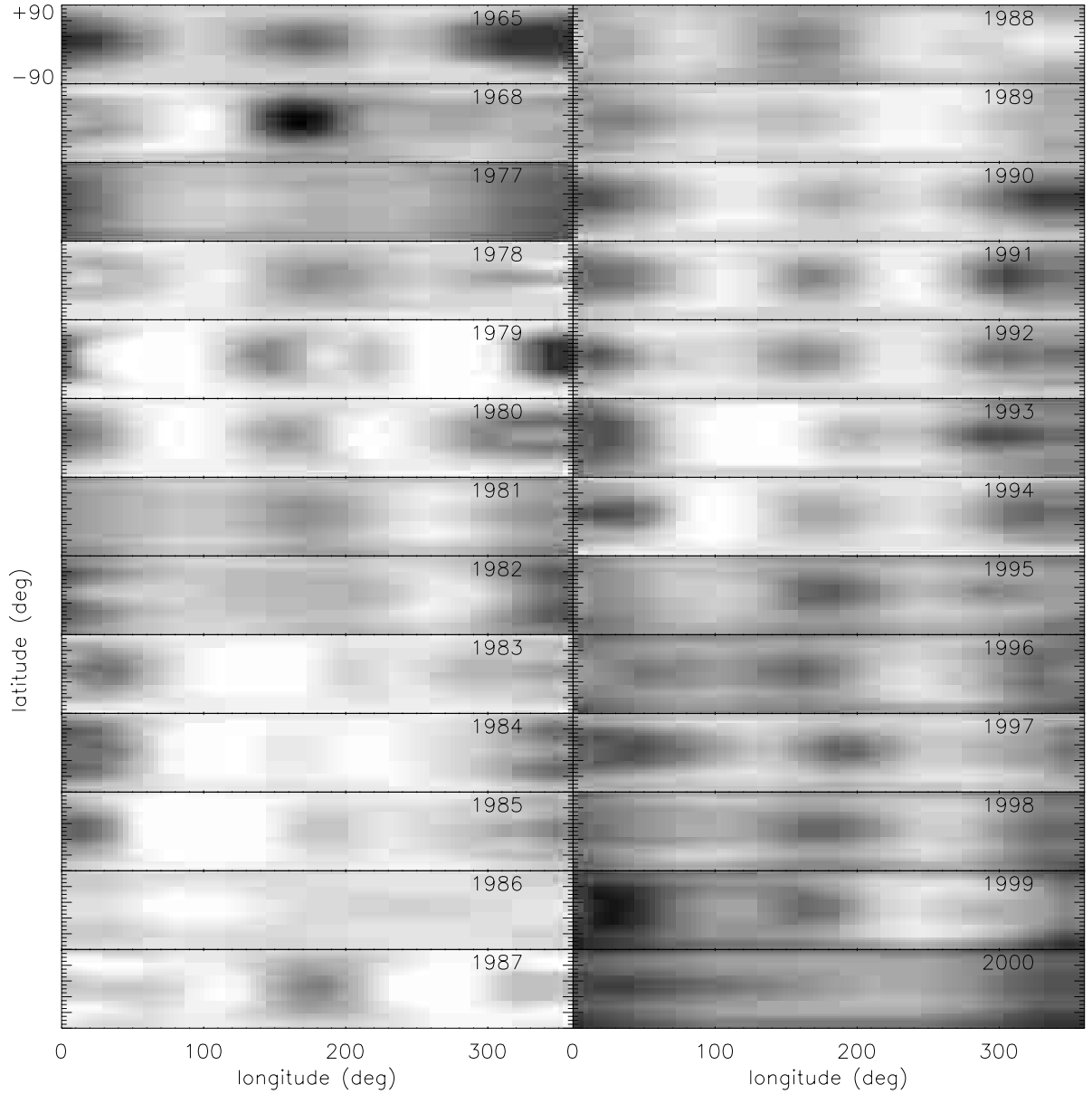
Fig. 6. The distribution of the spot covering factor on the more massive primary star from Maximum Entropy regularized fits of the *V*-band light curves from 1965 to 2000.

minimize the total spot area whereas the T models inevitably increases it by smoothing the surface variation of intensity; however, the time variations of the area obtained with the two different regularization criteria are very similar and the general variability trend can be regarded with confidence.

The data indicate a long-term change of the spot area suggesting a possible long-term cycle with a period of approximately 35 yr. Maxima were observed in 1965 and 2000, while a minimum was reached around 1985. A Fourier analysis based on the Scargle periodogram (Scargle 1982; Horne & Baliunas 1986) was applied to search for shorter term periodicity. After filtering the long-term trend, we found a period of 8.7 yr in the ME area variation with a confidence level of 98% and a period of 8.3 yr in the T area variation with a confidence

level of 81%. About three cycles of such a short-term modulation appear in our data, particularly in the variation of the unevenly distributed spotted area component (cf. Fig. 14c), supporting the existence of an activity cycle with a period of 8−10 yr.

The total spotted area on the G9 IV secondary showed a phase of sizeable variations in the 1977–1979 period, followed by an overall slow increase between 1981 and 2000. The coverage factor ranged from ∼8% to ∼20%, both for the ME and the T models, although for most of the time the spot coverage fraction was between 15% and 20% of the stellar surface. The Scargle periodogram did not show any significant periodicity in the spot area variation of the G9 IV star.

Our long-term sequence of data allows us to investigate the change of the longitudinal distribution of the

Fig. 7. The distribution of the spot covering factor on the more massive primary star from Tikhonov regularized fits of the V-band light curves from 1965 to 2000.

spotted area on each component of RT Lac. It is interesting to compare the longitude of the centroid of the spot distribution with the variation of the area of the unevenly distributed component, which determines the location of the centroid itself (cf. Fig. 16a, b for the primary, and Figs. 17a, b for the G9 IV secondary). The longitude of the centroid is defined as: $L_c = \int_0^{2\pi} a(l)l\,dl / \int_0^{2\pi} a(l)\,dl$, where $a(l) \equiv a_D(l) + a_U$ is the total spotted area in the longitude interval $[l, l + dl]$. We evaluated the integrals using the trapezium rule, computing L_c separately for the ME and T maps, and then averaging the two values.

On the primary component, we find evidence for a sudden change of the centroid longitude near the minima of the spot area in 1978 and 1987, whereas in the 1978–1987 period the longitude of the centroid migrated steadily at

an average rate of $\sim0.015°/$d in the direction opposite to the orbital motion. The sparse data during the 1965–1978 period might support the hypothesis of a regular migration of the centroid during that period. The large area fluctuations and the contemporary more random motion of the centroid during the 1989–2000 period, do not allow us to establish any clear correlation between them. In the entire 1965–2000 period, the migration rate varied from $\sim0.13°/$d in the direction of stellar rotation to $\sim0.10°/$d in the opposite direction. The amplitude of such a variation can be used to estimate the relative amplitude of the stellar differential rotation, giving: $\Delta\Omega/\Omega \sim 3.2\times10^{-3}$, which is about ten times smaller then the latitudinal differential rotation of the Sun in the sunspot belt (cf. Catalano 1983; LaBonte 1984) and quite consistent with the
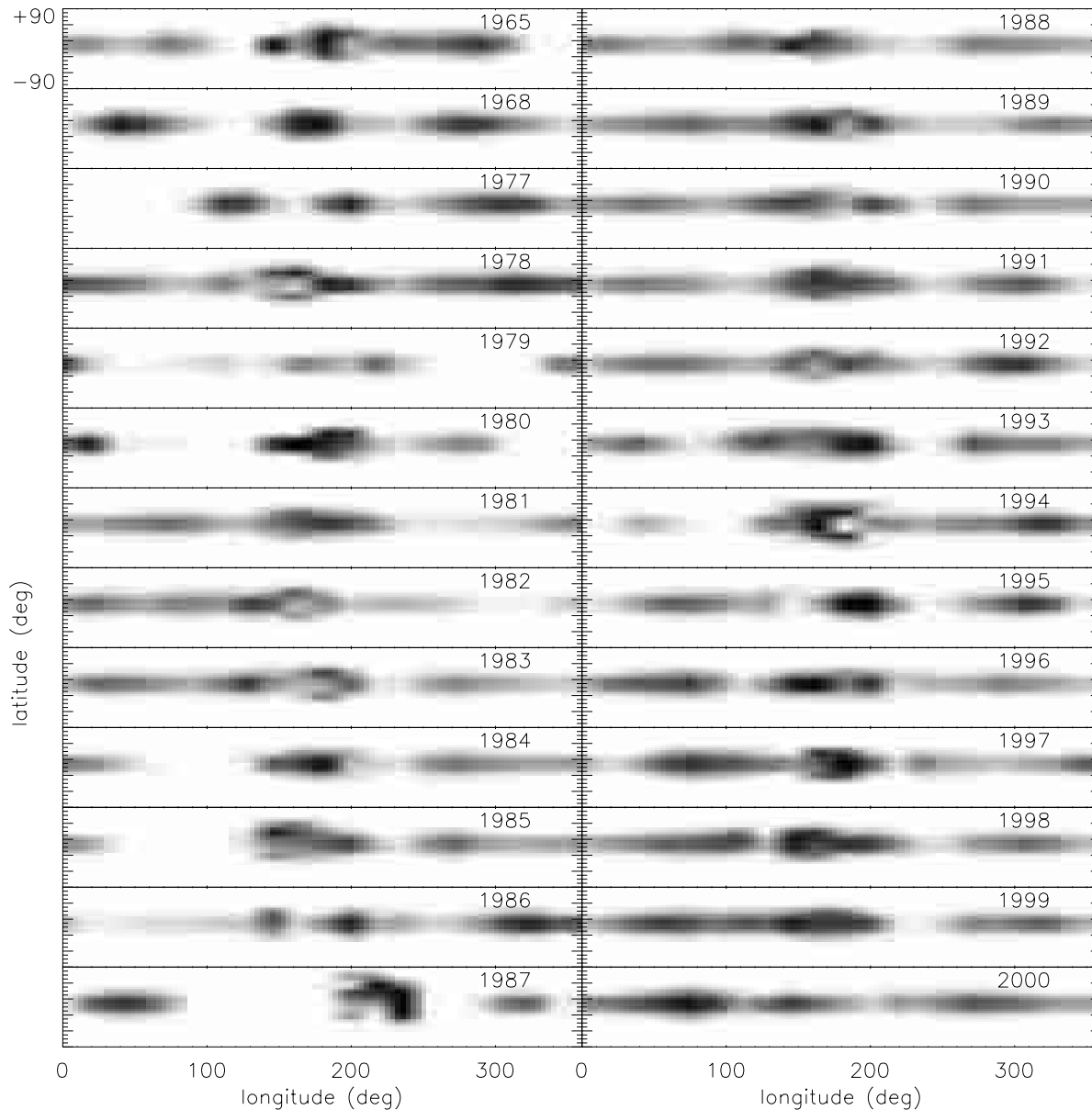
Fig. 8. The distribution of the spot covering factor on the G9 IV secondary from Maximum Entropy regularized fits of the *V*-band light curves from 1965 to 2000.

typical differential rotation rates that are obtained on other spotted stars (Hall 1991). It is important to note that the interpretation of the change of the migration rate of the centroid in terms of surface differential rotation is by no means unique. The same effect can be produced by a rearrangement of the spot pattern on a rigidly rotating star. Actually, an analysis of the 1978–1979 and 1987–1988 spot maps of the primary component shows that sizeable changes of the spot pattern took place and suggest that they may also contribute to the variation of the longitude of the centroid of the spot pattern.

The secondary star may also show cycles of migration of the centroid of its spot pattern with a period of approximately 10 yr, but the unevenly distributed spotted area stayed almost constant during those changes. The migration rate varied from ~0.11°/d in the direction of stellar

rotation to ~0.09°/d in the opposite direction, which may imply a relative amplitude of the differential rotation of $\Delta\Omega/\Omega \sim 2.7 \times 10^{-3}$.

5.3. Orbital period variation

The variation of the orbital period of RT Lac was recently investigated by Keskin et al. (1994) and Ibanoglu et al. (2001), who presented also the latest O–C diagram of the system (cf. their Fig. 6). It shows a long-term modulation with a period of approximately one century upon which a shorter term modulation is superposed. It is difficult to trace the long-term variation because of the large scatter of the O–C values based on old visual and photographic measurements, which have standard deviations of the order of 0.03−0.05 d. The short-term modulation is
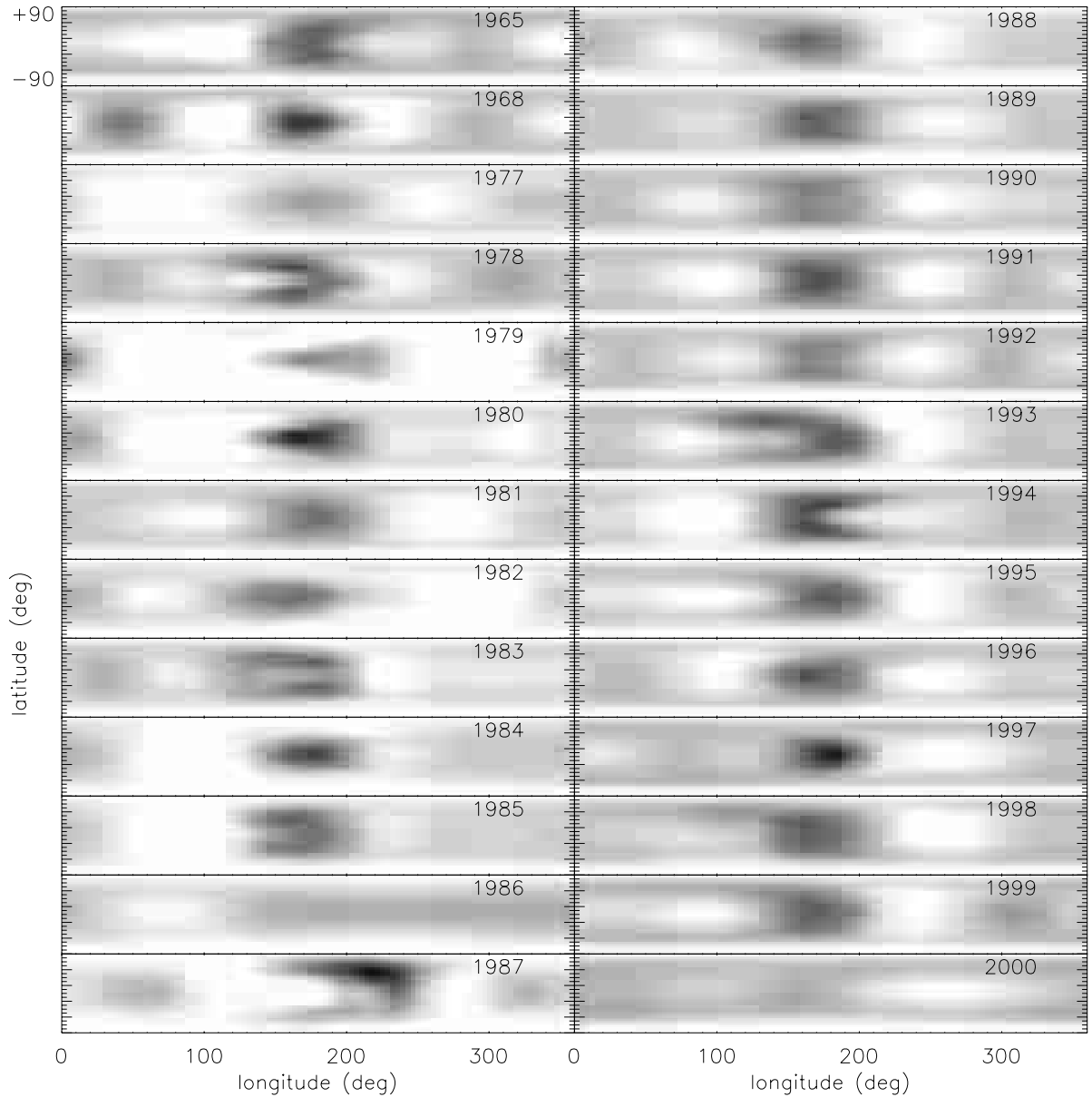
Fig. 9. The distribution of the spot covering factor on the G9 IV secondary from Tikhonov regularized fits of the V-band light curves from 1965 to 2000.

better defined, although a significant scatter is also present in the photoelectrically determined O–C with standard deviations of $\sim$0.01−0.015 d. The scatter is likely to be associated with the distortion of the eclipse ingress and egress light due to spot activity (cf. Hall & Kreiner 1980 for a discussion of such an effect) and it makes difficult to trace the orbital period change in great detail. In order to reduce the perturbation, the epochs of mid eclipse were determined using the points below the half depth of the eclipses, i.e., the nearly symmetric portion of the minima (cf. İbanoğlu et al. 2001 for the uncertainties of the epochs of the minima).

Secondary eclipses follow the same O–C variation of the primary eclipses, ruling out apsidal motion as a possible explanation for the period change.

After removing the long-term modulation, İbanoğlu et al. (2001) showed that the photoelectric O–C may be fitted by an approximately sinusoidal modulation with an amplitude of 0.028 d and a period of 17.8 yr. It is interesting to study the relationship of such a short-term modulation with the area and the migration of the spot pattern on the component stars, in view of the models recently proposed for the connection between magnetic activity cycles and orbital period modulation. The primary component is more likely to be responsible for the orbital period changes because it is the more active star and it shows clear evidence for an activity cycle. However, a possible role of the G9 IV secondary can not be excluded, hence we shall discuss also its spotted area variation in connection with the orbital period changes. In Fig. 18 we plot the total spotted area of the primary component, the longitude of the
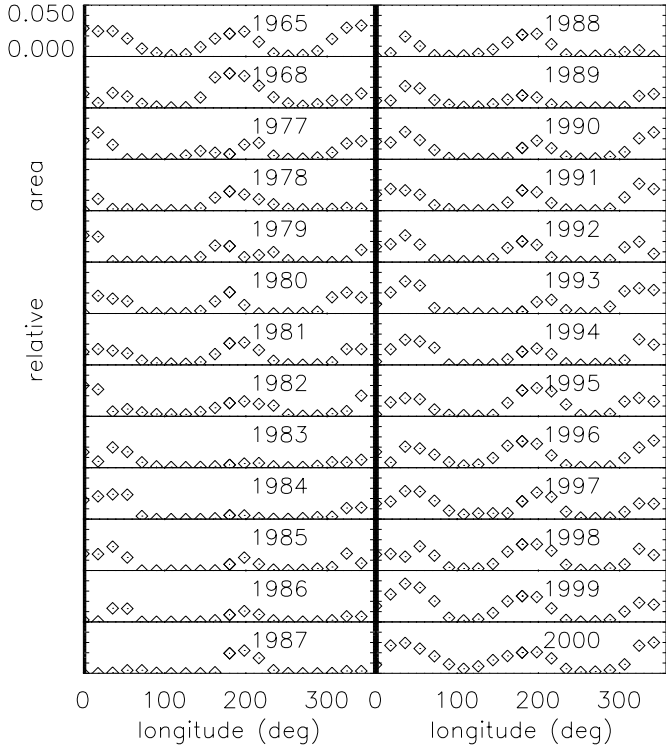
Fig. 10. The distribution of the relative spot area vs. longitude obtained from the ME models for the primary. The area unit is the area of the star photosphere (see text).
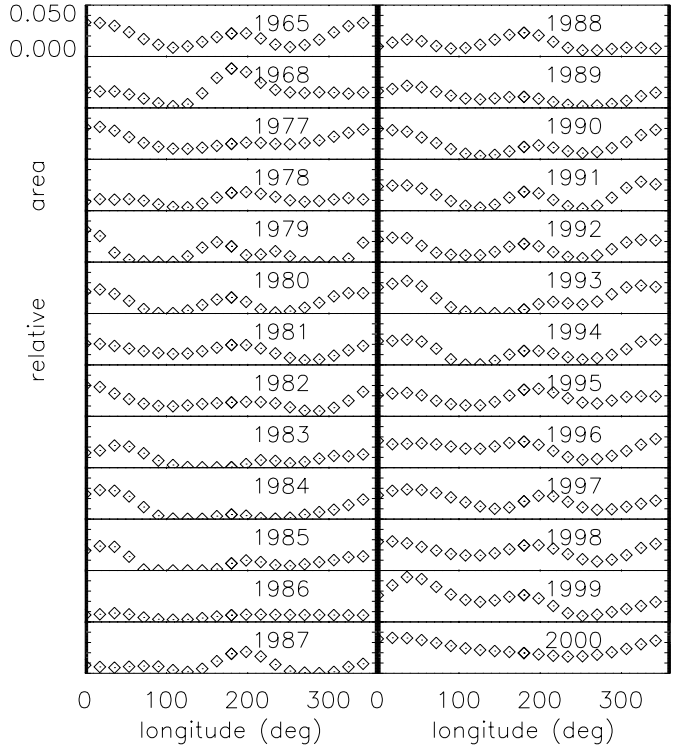

Fig. 11. The distribution of the relative spot area vs. longitude obtained from the T models for the primary. The area unit is the area of the star photosphere (see text).

centroid of its spot pattern and the O–C of the secondary eclipses, as defined according to the revised ephemerides in Table 1, on the same time scale. In Fig. 19 we present the same type of data for the G9 IV secondary. The observed times of minima were taken from Keskin et al. (1994) and İbanoğlu et al. (2001); the computed times were reckoned by means of the following linear ephemeris:

$$\text{Min } II = 2440382.8910 + 5.073945 \times E, \tag{4}$$

where E is the number of orbits elapsed from the initial epoch of secondary minimum and the new mean orbital period was derived from the photoelectrically determined O–C only. In the present analysis we did not plot primary minima in order to reduce the scatter of the O–C data (cf. İbanoğlu et al. 2001). Four time intervals of approximately constant orbital period can be identified and they are marked as I, II, III and IV in Figs. 18 and 19, respectively. In Table 4 we indicated the approximate beginning and end of each interval with the corresponding value of the orbital period and the relative variation with respect to the reference period of the ephemeris in Eq. (4).

The orbital period was longer than the reference period in the interval I, as indicated by the positive slope of the O–C diagram, then it decreased with a relative change of $\Delta P/P \sim 1.7 \times 10^{-5}$ around HJD 2444200. A further decrease occurred around HJD 2447200, at the end of interval II. Then the orbital period increased again around HJD 2449400, at the end of interval III. It is interesting to note that the episodes of orbital period decrease are

associated with relative minima of the spot coverage and possible increase of the rotation rate of the primary star. Conversely, the episode of orbital period increase at the transition between III and IV occurred during a phase of approximately constant spot coverage, that was immediately followed by a steep increase of the spot area. The longitude fluctuation of the centroid did not suggest any variation of the stellar rotation during the event.

The remarkable orbital period decrease around HJD 2444200 was accompanied by a sizeable decrease of the spotted area also on the G9 IV secondary. Its rotation rate might have accelerated as suggested by the decrease of the slope of the plot of L_c vs. time. The other episodes of orbital period change could not be related with sizeable change of the spotted area on the G9 IV component, which stayed approximately constant in the 1980–2000 period, fluctuating by a few per cents around its mean value. Different interpretations of the O–C diagram are also possible. For instance, a continuous parabolic fit could be applied to the variation that occurred between HJD 2439000 and 2449400, but we prefer the present model because it has a smaller reduced χ^2 than a continuous parabolic fit.

These observational results will be discussed in the next section in the light of the models recently proposed to relate magnetic activity and the perturbations of orbital dynamics in close binaries.
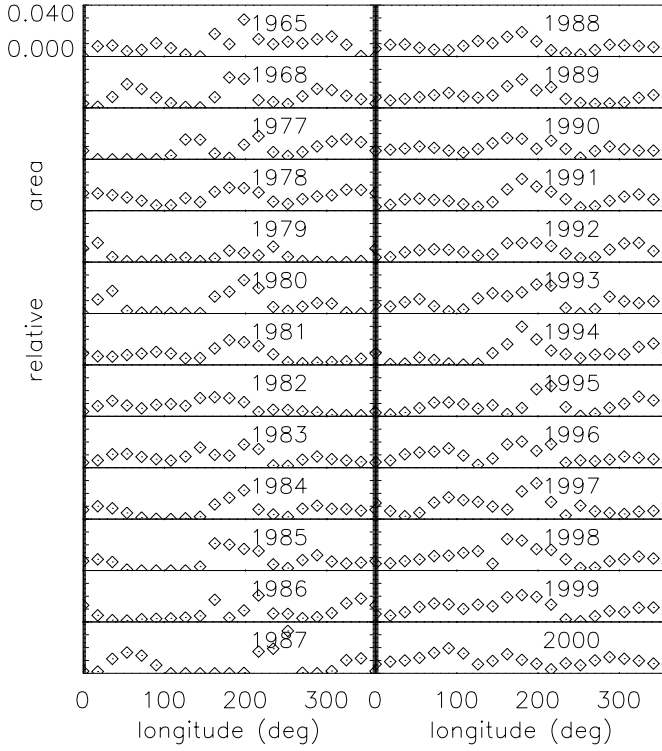
Fig. 12. The distribution of the relative spot area vs. longitude obtained from the ME models for the G9 IV secondary. The area unit is the area of the star photosphere (see text).
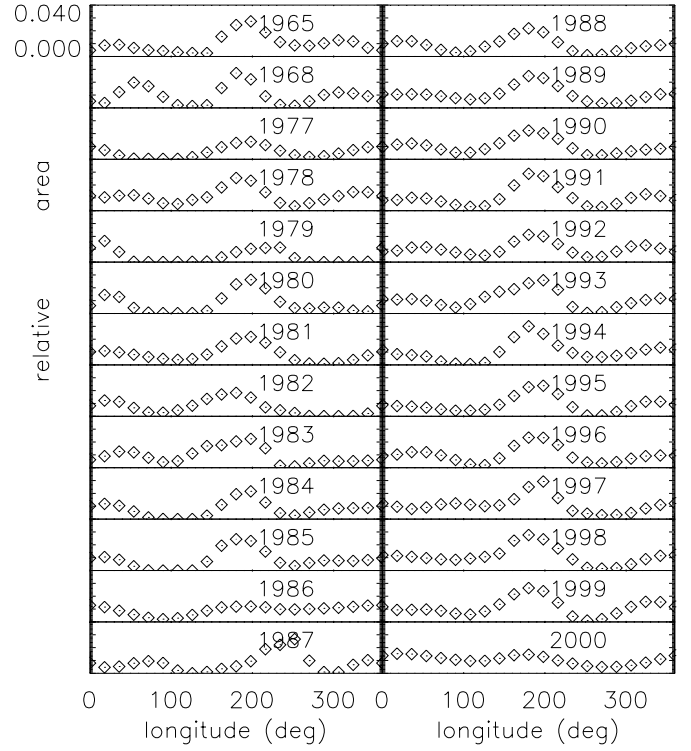

Fig. 13. The distribution of the relative spot area vs. longitude obtained from the T models for the G9 IV secondary. The area unit is the area of the star photosphere (see text).

Table 4. Orbital period variation of RT Lac.

Time Interval (HJD −2400000)	P (d)	$(P - P_{\rm ref})/P_{\rm ref}$
39000−44200	5.073987	$+8.29 \times 10^{-6}$
44200−47200	5.073900	-8.88×10^{-6}
47200−49400	5.073865	-1.57×10^{-5}
49400−52000	5.073939	-1.20×10^{-6}

6. Discussion

Our fitting procedure based on a spot model with fixed stellar parameters and constant spot temperature proved to be quite suitable to successfully model all the light curves in our sequence. The eclipse distortions were adequately modelled by adjusting the distribution of the spots over the surfaces of the components, without any need of varying the component relative radii which are evaluated with an accuracy of ±0.007. This precision is mainly limited by the light fluctuations close to minima because of the activity affecting the system (cf. Rodonò et al. 2001 for more details on the accuracy of the parameters derived by our model). We found no photometric evidence for the existence of an extended envelope around the primary component and of the required mass loss from the secondary to maintain it. The apparently anomalous color indexes of the primary and the infrared and ultraviolet excess of the system is likely due to the presence of cool spots, although a detailed multiband modelling of

the light curves of RT Lac has not been performed yet (cf. Hall 1989; Popper 1991).

Ibanoglu et al. (1998b) modelled the 1984 V-band light curve and the $B - V$ color curve simultaneously, with a circular spot on the hotter component in order to account for both the light curve distortions and the apparent color anomalies at the minima. The infrared photometry by Milone (1976) provided a coarse measure of the spectrum of the system infrared excess. It is interesting to estimate the contribution of the spots to the infrared excess by using a simplified model: the emergent flux from a spotted star in a given band is a linear combination of the fluxes from the spotted and unspotted photospheres, i.e., $F = (1 - f_{\rm D})F_{\rm U} + f_{\rm D}F_{\rm S}$, where $f_{\rm D}$ is the spot covering fraction of the disk at the given rotational phase and $F_{\rm U}$ and $F_{\rm S}$ are the flux from the unspotted and the spotted photospheres, respectively. An application to the Milone's (1976) analysis, by using the Johnson's (1966) color indexes to evaluate the surface flux ratios, shows that the infrared excesses are roughly: $\delta J \approx -0.086$, $\delta K \approx -0.15$ and $\delta L \approx -0.20$ mag when a temperature difference of 1000 K is assumed between the unspotted photosphere and the spots, and the average filling factors are $f_{\rm D} = 0.35$ and $f_{\rm D} = 0.20$ for the more massive and the less massive component, respectively. Such values of the infrared excesses compare well with the observed phase-dependent components of the excesses. However, they are too small to account also for their phase-independent components (cf. Milone 1976). Only if unrealistically large spot
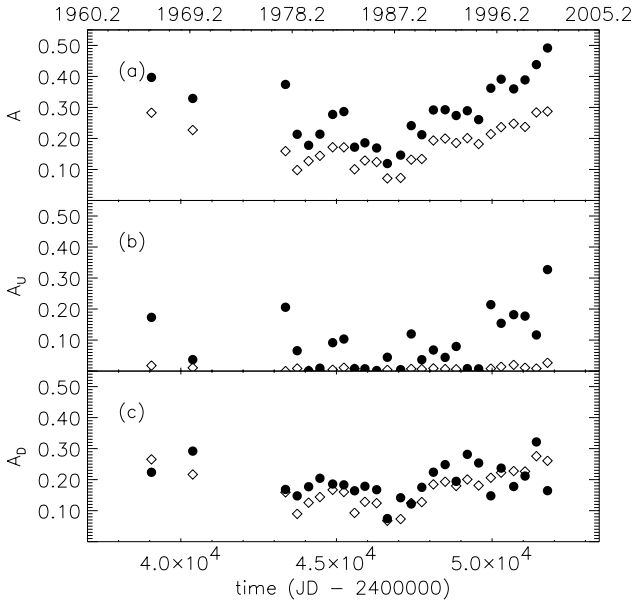
Fig. 14. a) The total spotted area A, **b)** the area of the uniform, evenly distributed spot component A_U, and **c)** that of the discrete, longitudinally dependent spot component A_D, vs. time for the more massive primary. The open symbols refer to the areas derived from the ME models, the filled symbols to the areas derived from the T models, respectively. The areas are normalized to the photospheric area of the primary component.

Fig. 15. a) The total spotted area A, **b)** the area of the uniform, evenly distributed spot component A_U, and **c)** that of the discrete, longitudinally dependent spot component A_D, vs. time for the G9 IV secondary. The open symbols refer to the areas derived from the ME models, the filled symbols to the areas derived from the T models, respectively. The areas are normalized to the photospheric area of the G9 IV component.

Fig. 16. a) The longitude of the centroid of the spot area distribution L_c and **b)** the area of the discrete, longitudinally dependent spot component A_D vs. time for the more massive primary.

filling factors were adopted ($f_D = 0.80$ for the more massive star and $f_D = 0.5$ for the less massive component), could the phase-independent components also be accounted for. Therefore, the possibility that these components are associated with circumstellar matter arising from mass loss or transfer processes can not be a priori excluded. Actually, Milone (1976, 1977) suggested that spot activity is not the only viable explanation for the photometric phenomenology shown by RT Lac and that mass loss or transfer may play a significant role.

Popper (1991) discussed the available spectroscopic data of RT Lac and concluded that the observed phenomenology is likely due to magnetic activity on the photospheres of the component stars rather than to mass transfer. Also Crawford (1992), although on the base of a limited amount of data, points in the same direction. However, the presence of circumstellar material and episodes of mass loss are well documented by the Hα observations of Huenemoerder (1985, 1988) and Huenemoerder & Barden (1986). It is difficult, however, to disentangle the line profile features due to chromospheric activity from those produced by mass loss to estimate the mass transfer rate in RT Lac (see, however, Frasca et al. 2002).

Mass loss and mass transfer have certainly played a fundamental role in the evolution of the system, as indicated by the study of Barrado et al. (1994), who found it impossible to fit the position of the two components on the H-R diagram with the same isochrone computed with
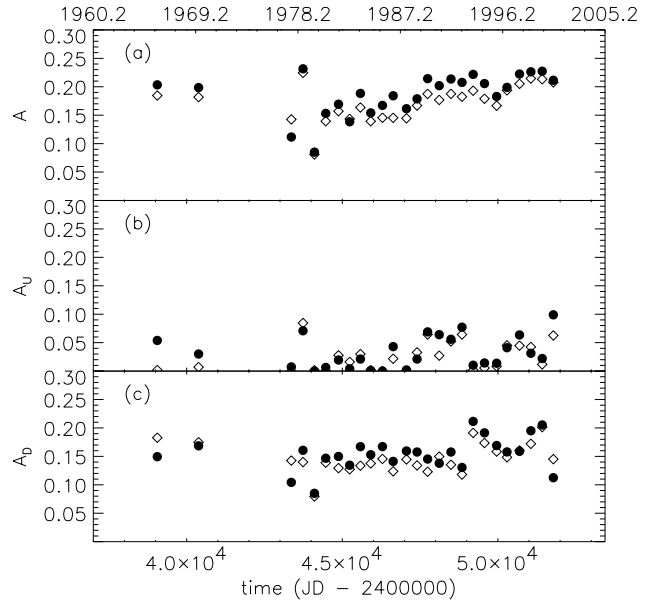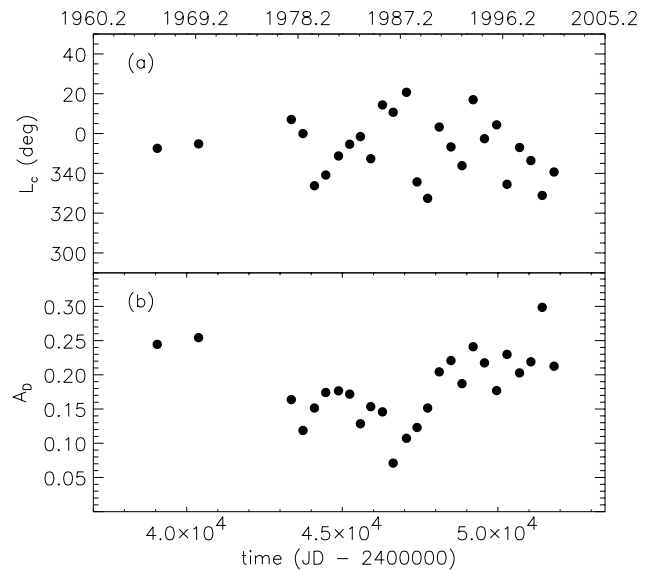
fixed stellar mass. Actually, the more evolved component of RT Lac is also the less massive star and the mass ratio is far from unity, indicating that the secondary has certainly experienced an intense mass loss or mass transfer toward the primary. Such processes may be related to a magnetized stellar wind, the intensity of which is
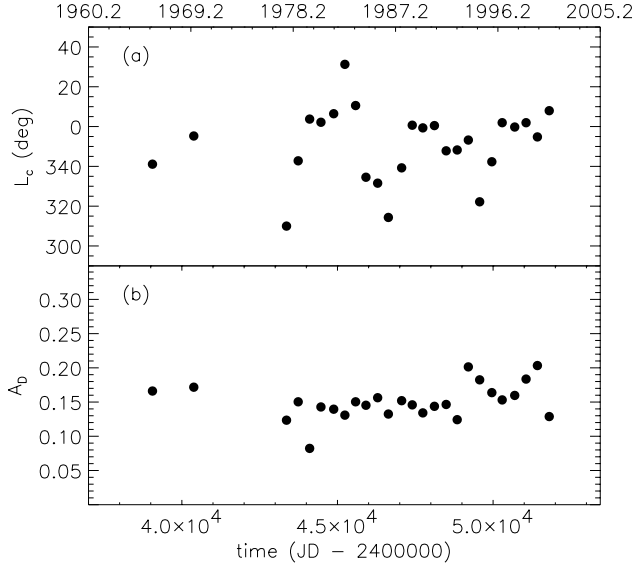
Fig. 17. a) The longitude of the centroid of the spot area distribution L_c and **b)** the area of the discrete, longitudinally dependent spot component A_D vs. time for the G9 IV secondary component.
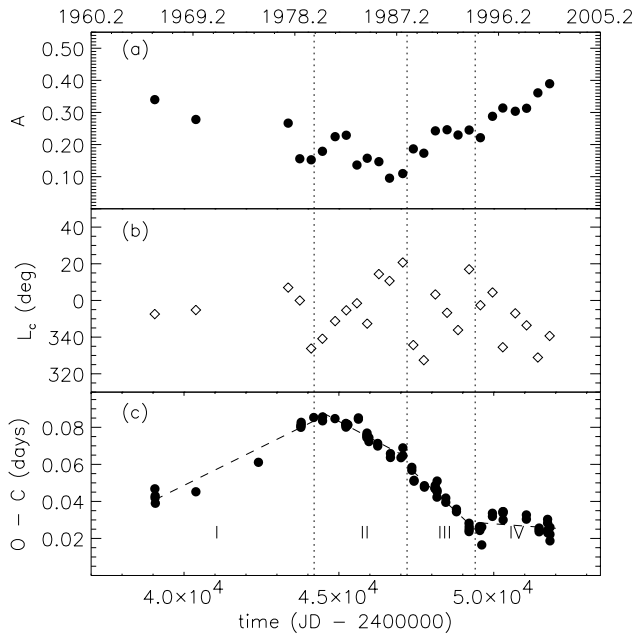

Fig. 18. a) The total spot area A (average between ME and T models) of the primary star, **b)** the longitude of the centroid of its spot pattern L_c and **c)** the O–C diagram vs. time. The four intervals of approximately constant orbital period described in the text are indicated in panel **c)** and the times of orbital period changes are marked by the dotted vertical lines. The dashed lines in panel **c)** are linear best fits to the O–C points during intervals of approximately constant orbital period.

expected to increase strongly when the star's surface closely approaches the Roche lobe (Tout & Hall 1991).

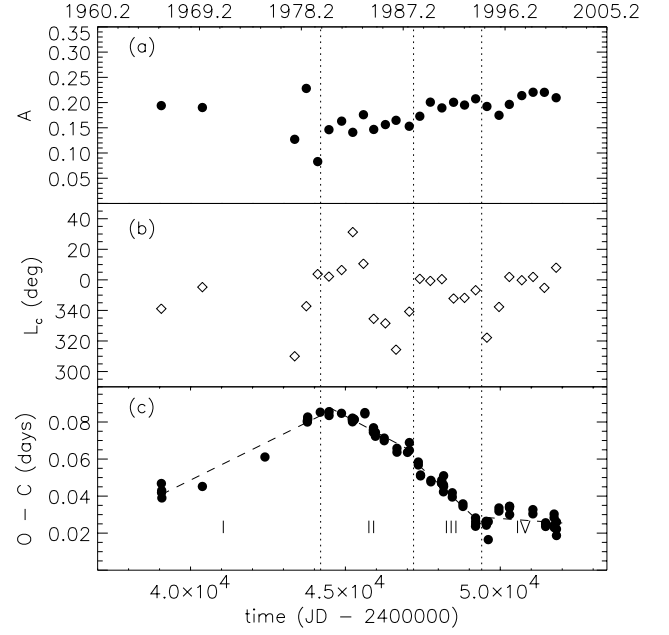Observational estimates of mass transfer rates in Algol binaries should be applicable also to RT Lac during

Fig. 19. a) The total spot area A (average between ME and T models) of the G9 IV secondary star, **b)** the longitude of the centroid of its spot pattern L_c and **c)** the O–C diagram vs. time. The four intervals of approximately constant orbital period described in the text are indicated in panel **c)** and the times of orbital period changes are marked by the dotted vertical lines. The dashed lines in panel **c)** are linear best fits to the O–C points during intervals of approximately constant orbital period.

its most intense episodes of mass transfer. Richards & Albright (1999) gives $10^{-11} < \dot{M} < 10^{-7} \ M_\odot/\mathrm{yr}$.

We can estimate the accretion luminosity L_{acc} due to the matter transferred from the lobe-filling secondary to the primary under the action of gravity as:

$$L_{\mathrm{acc}} = G\frac{M_1 \dot{M}}{R_1} \tag{5}$$

where M_1 and R_1 are the mass and the radius of the accreting primary and $\dot{M}$ is the accretion rate. If $\dot{M} = 10^{-8} \ M_\odot/\mathrm{yr}$, it yields: $L_{\mathrm{acc}}/L_V = 8 \times 10^{-3}$, where L_V is the luminosity of the system in the V-band, assuming the Hipparcos distance of 193 pc. Hydromagnetic effects are unlikely to change the order of magnitude of the estimates based on Eq. (5) (cf. Bolton 1989; Richards 1992). Therefore, the effect of mass transfer should be negligible in comparison with the variations due to the spot activity in wide-band photometry, except when the highest mass loss rate of Algols is approached.

The luminosity ratio in the V passband was determined through an optimization procedure using the light curves with the most complete phase coverage, as already done for RS CVn and AR Lac in previous papers (cf. Rodonò et al. 1995; Lanza et al. 1998a). The value we found, $L_1/L_2 = 0.65 \pm 0.05$, compares well with the estimate by Milone (1977), who found $L_1/L_2 = 0.70$. He used the Russell model to determine the binary system

parameters after removing as well as possible the effect of the distortion wave by a simple rectification procedure.

It is important to note that our approach is to fit all the light curves in our sequence using the same unspotted luminosity ratio, i.e., that corresponding to the components without spots on their photospheres. Other authors have chosen to include the luminosity ratio among the model parameters, allowing it to change from one light curve solution to another (e.g., Kang & Wilson 1989). We prefer a constant value because it is unlikely that the effective temperatures of the unspotted photospheres change on timescales of a few decades (Spruit 1982; Spruit & Weiss 1986). It should be noted that the value of the unspotted luminosity ratio we determine in the present analysis depends on the value adopted for the unspotted magnitude of the system, that in our case is the magnitude at the maximum brightness ever observed. Its dependence on other photometric parameters is much smaller and it was not investigated in the present study because we do intend to focus on the analysis of the magnetic activity. More information can be found in Rodonò et al. (2001), where a method for the simultaneous determination of the luminosity ratio and other photometric parameters (relative radii, orbital inclination, etc.) is presented.

The information content of the light curves is adequate to characterize the main features of the spot activity on both components of RT Lac. We applied simultaneously two different regularization techniques in order to point out which features are actually needed by the data and which are artifacts of the regularization itself. As already noted by Lanza et al. (1998a), the application of ME and T techniques to photometric data produces results that require a more careful interpretation than in the case of the Doppler Imaging maps, which are based on high-resolution spectroscopic data with an intrinsically greater information content. Even in the case of light curves with an ideal phase coverage and infinite signal-to-noise ratio, the regularization techniques introduce artifacts. In the case of the ME regularization they mainly consist of the so-called *super-resolution*, i.e., the presence of compact and highly contrasted features on the maps which can not be actually resolved by means of photometric techniques. On the contrary, the T regularization tends to produce uniformly spotted grey areas in those regions that do not contribute significantly to the light curve modulation, such as the polar regions in an eclipsing system, that are strongly subject to foreshortening. A detailed description of the causes of such artifacts can be found in Lanza et al. (1998a). From these arguments, it is not possible to specify an ideal regularizing criterion for wide-band light curve analysis. In our opinion, the best approach is to regard regularized maps as an intermediate stage of the analysis and use them only to derive quantities which do not depend on the regularizing criterion itself, e. g., the spot longitudes, their changes in time and the variations of the total spotted area. Absolute values of the spotted areas are not reliable since they depend on the unspotted magnitude and the regularizing

criterion adopted, but their time variations show a very small dependence on both of them.

The spot activity on the more massive primary is localized in two main active regions around longitudes $0°$ and $180°$, respectively. There may be some tendency for activity to switch alternatively from one active longitude to the other from time to time, but the phenomenon is not as clearly apparent as in, e.g., II Peg (Rodonò et al. 2000) or other RS CVn binaries (Berdyugina & Tuominen 1998). The active region around the substellar point on the primary sometimes shows the presence of a compact spot with a diameter of $\sim 40°$, comparable with the resolution limit of the eclipse mapping technique. It appears in the maps of some of the best covered light curves (e.g., 1985, 1999) and suggests that even smaller, probably solar-size spots, may be present on the photosphere of the primary star.

The G9 IV secondary shows spot activity more uniformly distributed in longitude, although a quite compact active region around the substellar point is often present. On the T maps it is the most prominent feature together with another active longitude located on the opposite hemisphere, which is broader and less contrasted.

The presence of active longitudes is a common phenomenon on RS CVn binaries (e.g., Henry et al. 1995; Oláh et al. 1997; Rodonò et al. 2000). The concentration of activity around the substellar points on both components is well documented also by the cases of AR Lac and SZ Psc (Lanza et al. 1998a; Lanza et al. 2001). Mean field dynamo models predict the possible existence of active longitudes related to non-axisymmetric modes when the amplitude of the stellar differential rotation does not exceed about half the solar value. Only non-axisymmetric field geometries with an azimuthal wavenumber $m = 1$ have been found to be stable, but such a result may possibly be due to the many simplifying assumptions of present mean field models (Rädler et al. 1990; Moss et al. 1991; Rüdiger & Elstner 1994; Moss et al. 1995). Moreover, it is possible that the binary nature of the RS CVn's has an influence on the activity of the single components (Schrijver & Zwaan 1991). The mean field models by Moss & Tuominen (1997) show that the magnetic field tends to concentrate along the line connecting the two components in close binaries, in general agreement with our findings for AR Lac, SZ Psc and RT Lac. Moreover, the presence of preferential longitudes may be related to perturbations of the magnetic fields stored at the base of the convective envelopes, due to tidal forces, which eventually trigger the emergence of magnetic flux tubes (cf., e.g., Holzwarth & Schüssler 2000).

The spot patterns on the components of AR Lac and SZ Psc do not show a regular migration in time, whereas we have evidence for an oscillation of the longitude of the spot pattern centroid in the components of RT Lac. The rates of migration have been used to derive information on stellar differential rotation. The method provides us only with a lower limit for the amplitude of the differential rotation. Photometric data do not allow us to establish whether we are measuring the amplitude of the

latitudinal differential rotation or a possible time variation of the mean rotation rate of the photosphere, as required by some models of the orbital period change (see below). As a matter of fact, a change of the longitude of the centroid and of its rotation rate may also be produced by a rearrangement of the spot pattern without any variation of the rotation rate of the photosphere. Therefore, our estimates of the differential rotation rate and of its possible time variations can not be regarded as conclusive.

Moreover, the measurement of differential rotation can be a difficult task when permanent active longitudes are present, as showed by, e.g., Eaton et al. (1996). Measuring the period of the rotational modulation is a more suitable tool to study stellar differential rotation, even in the case of complex active longitude behaviour, as shown by, e.g., Rodonò et al. (2000). Their approach works well for non-eclipsing systems, but in our case the light modulation due to eclipses dominates, making it difficult to extract the rotational modulation of the individual stars (cf. Lanza et al. 1994).

Polar spots are not required by our solutions, but this leaves unanswered the question of their existence, claimed by several authors (see, however, Hatzes et al. 1996 and Hatzes 1998 for a critical discussion of the related spectroscopic evidence). The presence of large low-latitude spots, as deduced by our eclipse mapping, is a significant constraint for dynamo models. It suggests the existence of MGauss toroidal fields in the overshoot region below the convective envelope of the secondary component (Schüssler & Solanki 1992; Schüssler et al. 1996; Granzer et al. 2000). Toroidal flux tubes with field strengths exceeding $(2-4) \times 10^6$ G should have unstable modes with azimuthal order $m = 1$ or $m = 2$, whose subsequent nonlinear evolution can be quite complex (Caligari et al. 1995; Schüssler et al. 1996). Alternatively, a distributed dynamo operating in the bulk of the convective envelope might be invoked to explain low-latitude activity.

In this scenario, the flux tubes might emerge near the equator in spite of the large Coriolis force because they are produced in layers not too far from the surface.

The time evolution of the spotted area on the primary component shows a short-term cycle with a period of about 8–9 yr and a longer term change with a period of approximately 35 yr. A short-term cycle with a period of ∼10 yr was already suggested by Ibanoglu et al. (2001) who analysed the variation of the magnitude at the center of the secondary eclipse, when the primary is in view. The observations of other RS CVn binaries show that the periods of the activity cycles are typically between one and two decades, so that a cycle of $8-10$ yr in the primary component of RT Lac compares well with the general behaviour of that class (Henry et al. 1995; Rodonò et al. 1995; Lanza et al. 1998a; Saar & Brandenburg 1999; Oláh et al. 2000). It is interesting to note that the rearrangements of the spot pattern with possible accelerations of the spot rotation rate on the primary star in 1978 and 1987 were associated with minima of the total spotted area, i.e., the beginning of a new activity cycle. Such a behaviour is indeed reminiscent of the solar cycle phenomenology and it has been reported also in other stars (cf. Messina et al. 1999; Rodonò et al. 2000). However, given the lack of information on starspot latitudes, it is difficult to explore in more detail the connection.

We can use the decrease of the total spotted area observed between 1977 and 1978 to estimate the turbulent magnetic diffusivity η_t in the convective envelope of the primary star, as done by, e.g., Lanza et al. (1998a) for the secondary of AR Lac, in the hypothesis that the variation is due only to the decay of the magnetic field. Adopting a radius of 4.4 $R_\odot$ and estimating $\eta_t \approx \Delta A / \Delta t$, where ΔA is the decrease of the spot area in the time interval Δt, we find: $\eta_t \sim 4 \times 10^{11}$ m^2 s^{-1}. For the G9 IV secondary having $R = 4.8$ $R_\odot$, we find: $\eta_t \sim 6 \times 10^{11}$ m^2 s^{-1}. They are comparable to the value estimated for the K2 IV secondary of RS CVn (Rodonò et al. 1995). Such values are more than 100 times larger than in the Sun, but they are not unreliable since on a G subgiant we expect that the mixing length and the velocity of the turbulent convection may be significantly larger than in the Sun (Schwarzschild 1975). An estimate based on the convective envelope models by Rucinski & Vandenberg (1986) provides values of η_t within an order of magnitude of the observationally estimated values.

The orbital period change of RT Lac was investigated by Keskin et al. (1994) and Ibanoglu et al. (2001) who found little support for a light-time effect interpretation, that assume the orbital motion of the system around a third body. The third body should have a minimum mass of ∼1.25 $M_\odot$ and thus its effects on the light curves and the spectra of the system would be easily detectable. Moreover, the claimed variation of the radial velocity of the barycenter of the couple, if real, is not in agreement with the derived orbital period of about one century for the orbit of the third body.

The possibility that the orbital period change is due to mass transfer is ruled out by the alternate sign of the modulation. Indeed, conservative mass transfer from the less massive lobe-filling secondary toward the primary should steadily increase the orbital period, contrary to the observations. Moreover, the mass transfer rate should amount to a few 10^{-5} $M_\odot$/yr, which appears to be too large in comparison with the $10^{-11}-10^{-7}$ $M_\odot$/yr value that is typical of Algol binaries (cf., e.g., Richards & Albright 1999), and spectroscopic evidence of such a huge mass transfer rate is solely lacking (cf. also Frasca et al. 2002).

Therefore, the only mechanism that seems capable of explaining both the short- and the long-term modulation of the orbital period of RT Lac is that proposed by Applegate (1992) and recently revisited by Lanza et al. (1998b) and Lanza & Rodonò (1999). It connects the changes of the orbital period with the variation of the gravitational quadrupole moment of the active star, produced by a powerful hydromagnetic dynamo. Applegate (1992) assumed that the angular momentum of the outer layers of the convection zone of the star varies cyclically because of the angular momentum exchanges produced

by magnetic stresses along the activity cycle. Lanza et al. (1998b) and Lanza & Rodonò (1999) pointed out the possible role of the Lorentz force in the variation of the figure of equilibrium of the star, which helps to reduce the amplitude of the angular velocity and kinetic energy variations required by the mechanism. Their approach is general and independent of the specific dynamo model applied to the star, because it makes use of Chandrasekhar's virial theorem to estimate the kinetic and magnetic energy changes associated with the observed period variation. Assuming that the sum of the kinetic energy of rotation and of magnetic energy stays constant during an activity cycle, Lanza & Rodonò's (1999) model predicts that the orbital period should be at a minimum when the kinetic energy of rotation is maximum and the magnetic energy is minimum. The results of Sect. 5.3 supports this prediction because the two episodes of orbital period decrease occurred during minima of activity and were accompanied by a migration of the centroid of the spot pattern in the direction of stellar rotation on the primary component that may indicate an acceleration of the rotation rate of its outer convection zone. In the 1978 orbital period decrease, also the secondary star might have played a role because it also showed a marked decrease of spot area and a migration of the centroid of the spot pattern in the direction of stellar rotation. Conversely, the increase of the orbital period in 1993 was associated with an increase of the magnetic energy, as witnessed by the increase of the spotted area on the primary component. The timescales for the orbital period variations derived from the O–C plots in Figs. 18 and 19 are of a few years and put strong constraints on the theoretical models of the process. More precisely, such rapid orbital period changes suggest that the main responsible for the variation of the stellar quadrupole moment should be the Lorentz force, because a variation of the angular momentum distribution on such short timescales would imply extremely large magnetic torques in the convective envelope of the active component. Therefore, the present observations would give more support to the models proposed by Lanza et al. (1998b) and Lanza & Rodonò (1999) than to the original mechanism proposed by Applegate (1992).

It is also of interest to compare the RT Lac's behaviour with those of the prototype RS CVn and SZ Psc. The observations of RS CVn supports the association between an orbital period decrease and an increase of the migration rate of the spots at a minimum of the activity cycle. The observations of SZ Psc indicate that an orbital period increase is associated with an increase of the spotted area, i.e., of the magnetic energy. Therefore, we conclude that the qualitative prediction of the model by Lanza & Rodonò (1999) is supported by the observations of these three active close binaries.

The observed amplitude of the orbital period variation can be used to estimate the variation of the kinetic energy of rotation and of the magnetic energy during the change, neglecting the consequences of the short timescales required by the observations for the angular momentum exchanges.

The episode of orbital period decrease that occurred in 1978 implied an increase of the kinetic energy of rotation of $\sim 6.5 \times 10^{36}$ J for the primary and of $\sim 8.0 \times 10^{35}$ J for the secondary star, assuming that both played comparable roles in the variation. The corresponding relative increases of the rotation rate are $\Delta\Omega/\Omega \sim 8.0 \times 10^{-3}$ for the primary and $\Delta\Omega/\Omega \sim 2.2 \times 10^{-3}$ for the secondary star. The observed relative change of the migration rate of the spots is significantly lower for the primary and comparable with the predicted value for the secondary. However, active region evolution and the presence of active longitudes may affect the measured migration rate, altering the amplitude of their change.

An episode of orbital period increase occurred in 1993 and implied an increase of the magnetic energy of the active primary of $\sim 1.1 \times 10^{37}$ J, which may be associated with a mean field of $\sim 1.5 \times 10^{5}$ G in the convection zone of the star. Such a high field is indeed strongly unstable to magnetic buoyancy, unless is it organized in the form of vertical flux tubes (cf. Lanza & Rodonò 1999). Unstable fields that buoyantly rise through the convective envelope and experience the effects of the Coriolis force, may produce a new kind of α-effect that makes the stellar dynamo capable of working even when the conventional α-effect is severely quenched (Brandenburg & Saar 2000). Such a magnetically driven α-effect might account for the strong fields that are required to produce the variation of the quadrupole moment and the low-latitude spot activity in the secondaries of RS CVn binaries.

An interesting result of our analysis is that the activity cycle of the primary star has a period of ~ 9 yr, i.e., half that of the short-term orbital period change found by Ibanoglu et al. (2001). Rodonò et al. (1995) and Lanza et al. (1998a) found a similar phenomenon also in RS CVn and AR Lac, respectively. Lanza et al. (1998b) proposed that such a behaviour may be associated with a torsional oscillation excited by the non-linear stellar dynamo. However, the predicted phase relation between the oscillation of the orbital period, the rotation rate and the spot area does not seem to be observed in RT Lac. The time span of the data is indeed too short to draw a definite conclusion on this point, also because the fluctuations of the spot area and the presence of active longitudes may hide or alter the phase relationship among the variations. Thus, the possibility that torsional oscillations are responsible for the short-term modulation of the activity level in close active binaries, although quite plausible, remains to be demonstrated.

7. Conclusions

Our analysis of an extended sequence of light curves of RT Lac has led to several remarkable results. Our modelling approach based on Roche geometry and Kurucz's atmospheric models proved to be capable of fitting all of the light curves and, by using the ME and T regularizing

criteria, has provided us with maps of the spot covering factor. Moreover, taking into account the photometric effect of the spots, a consistent value of the V-band luminosity ratio between the two components was determined.

During the 1965–2000 interval, we do not find evidence for a variation of the relative radii of the components larger than ± 0.007, nor for a change of their shape, that can affect the ellipticity coefficients introduced in old light curve rectifications. Thus the variation claimed by Eaton & Hall (1979) on the basis of the analysis of old visual and photographic light curves is clearly liable to serious questionings.

The light curve analysis has given us information on the spot pattern showing, in particular, spots at low and intermediate latitudes and persistent active regions around the substellar points on both components. Our eclipse mapping shows the presence of rather compact spots on the occulted hemisphere of the primary star, with a diameter of $\sim 40°$ or possibly smaller.

The orbital period modulation appears to be correlated with spot activity on the component stars, in particular on the more massive primary. A detailed comparison between the spot area, the migration rate of the spot pattern and the orbital period change was possible for the 1965–2000 period. Our results give support to the model proposed by Lanza & Rodonò (1999) for the interpretation of the orbital period modulation in active close binaries.

References

Allen, C. W. 1973, Astrophysical Quantities (The Athlone Press, London)

Applegate, J. H. 1992, ApJ, 385, 621

Barrado, D., Fernández-Figueroa, M. J., Montesinos, B., & De Castro, E. 1994, A&A, 290, 137

Berdyugina, S. V., & Tuominen, I. 1998, A&A, 336, L25

Bolton, C. T. 1989, Space Sci. Rev., 50, 311

Brandenburg, A., & Saar, S. H. 2000, in Stellar clusters and associations: convection, rotation and dynamos, ed. R. Pallavicini et al., ASP Conf. Ser., 198, 381

Caligari, P., Moreno-Insertis, F., & Schüssler, M. 1995, ApJ, 441, 886

Catalano, S. 1983, in Activity in Red Dwarf Stars, ed. P. B. Byrne, & M. Rodonò (D. Reidel Publ. Co., Dordrecht), 343

Crawford, J. 1992, Dissertation, San Diego State Univ.

Dempsey, R. C., Linsky, J. L., Fleming, T. A., & Schmitt, J. H. M. M. 1993, ApJS, 86, 599

Diaz-Cordoves, J., Claret, A., & Gimenez, A. 1995, A&AS, 110, 329

Eaton, J. A., & Hall, D. S. 1979, ApJ, 227, 907

Eaton, J. A., Henry, G. W., Bell, C., & Okorogu, A. 1993, AJ, 106, 1181

Eaton, J. A., Henry, G. W., & Fekel, F. C. 1996, ApJ, 462, 888

Evren, S. 1989, Ap&SS, 161, 303

Evren, S., Tunca, Z., İbanoğlu, C., & Tumer, O. 1985, Ap&SS, 108, 383

Frasca, A., & Catalano, S. 1994, A&A, 284, 883

Frasca, A., Cakirli, O., Catalano, S., et al. 2002, A&A, in press

Gibson, D. M., Owen, F. N., & Hjellming, R. M. 1978, PASP, 90, 751

Granzer, Th., Schüssler, M., Caligari, P., & Strassmeier, K. G. 2000, A&A, 355, 1087

Gull, S. F., & Skilling, J. 1984, in Indirect Imaging, ed. J. A. Roberts (Cambridge Univ. Press, Cambridge), 267

Hall, D. S. 1976, in Multiple Period Variable Stars, ed. W. S. Fitch, IAU Coll. 29, 287

Hall, D. S., & Haslag, K. P. 1976, in Multiple Periodic Variable Stars, ed. W. S. Fitch, IAU Coll. 29, 331

Hall, D. S. 1989, Space Sci. Rev., 50, 219

Hall, D. S. 1991, in The Sun and Cool Stars: Activity, Magnetism, Dynamo, ed. I. Tuominen, D. Moss, & G. Rüdiger (Springer-Verlag, Berlin), 353

Hall, D. S., & Kreiner, J. M. 1980, Acta Astron., 30, 388

Haslag, K. P. 1977, Master Thesis, Vanderbilt Univ., Nashville, Tennessee

Hatzes, A. 1998, A&A, 330, 541

Hatzes, H. A., Vogt, S. S., Ramseyer, T. F., & Misch, A. 1996, ApJ, 469, 808

Henry, G. W., Eaton, J. A., Hamer, J., & Hall, D. S. 1995, ApJS, 97, 513

Holzwarth, V., & Schüssler, M. 2000, AN, 321, 175

Horne, J. H., & Baliunas, S. L. 1986, ApJ, 302, 757

Huenemoerder, D. P. 1985, AJ, 90, 499

Huenemoerder, D. P. 1988, PASP, 100, 600

Huenemoerder, D. P., & Barden, S. C. 1986, AJ, 91, 583

İbanoğlu, C., Evren, S., Taş, G., Devlen, A., & Çakırlı, Ö. 2001, A&A, 371, 626

İbanoğlu, C., Kurutac, M., Tumer, O., Evren, S., Tunca, Z., & Ertan, A. Y. 1980, Ap&SS, 72, 61

İbanoğlu, C., Pekünlü, E. R., Keskín, V., et al. 1998a, Ap&SS, 257, 11

İbanoğlu, C., Pekünlü, E. R., Keskín, V., et al. 1998b, Ap&SS, 257, 83

Johnson, H. L. 1966, ARA&A, 4, 193

Kang, Y. W., & Wilson, R. E. 1989, AJ, 97, 848

Keskin, V., İbanoğlu, C., Akan, M. C., Evren, S., & Tunca, Z. 1994, A&A, 287, 817

Kopal, Z. 1959, Close Binary Systems (Chapman & Hall Ltd., London)

Kopal, Z. 1989, The Roche Problem (Kluwer Ac. Publ., Dordrecht)

Kurucz, R. 2000 [http://cfaku5.harvard.edu]

LaBonte, B. J. 1984, ApJ, 276, 335

Lampton, M., Margon, B., & Bowyer, S. 1976, ApJ, 208, 177

Lanza, A. F., Catalano, S., Cutispoto, G., Pagano, I., & Rodonò, M. 1998a, A&A, 332, 541

Lanza, A. F., & Rodonò, M. 1999, A&A, 349, 887

Lanza, A. F., Rodonò, M., Mazzola, L., & Messina, S. 2001, A&A, 376, 1011

Lanza, A. F., Rodonò, M., & Rosner, R. 1998b, MNRAS, 296, 893

Lanza, A. F., Rodonò, M., & Zappalà, R. A. 1994, A&A, 290, 861

Maltby, P. 1992, in Sunspots: Theory and Observations, ed. J. H. Thomas, & N. O. Weiss (Kluwer Ac. Publ., Dordrecht), 103

Messina, S., Guinan, E. F., Lanza, A. F., & Ambruster, C. 1999, A&A, 347, 249

Milone, E. F. 1976, ApJS, 31, 93

Milone, E. F. 1977, AJ, 82, 998

Moss, D., Tuominen, I., & Brandenburg, A. 1991, A&A, 245, 129

Moss, D., Barker, D. M., Brandenburg, A., & Tuominen, I. 1995, A&A, 294, 155

Moss, D., & Tuominen, I. 1997, A&A, 321, 151

Narayan, R., & Nityananda, R. 1986, ARA&A, 24, 127

Oláh, K., Kolláth, Z., & Strassmeier, K. G. 2000, A&A, 356, 643

Oláh, K., Kövari, Zs., Bartus, J., et al. 1997, A&A, 321, 811

Piskunov, N. E., Tuominen, I., & Vilhu, O. 1990, A&A, 230, 363

Popper, D. M. 1991, AJ, 101, 220

Rädler, K.-H., Wiedemann, E., Brandenburg, A., Meinel, R., & Tuominen, I. 1990, A&A, 239, 413

Richards, M. T. 1992, ApJ, 387, 329

Richards, M. T., & Albright, G. E. 1999, ApJS, 123, 537

Rodonò, M., Lanza, A. F., & Catalano, S. 1995, A&A, 301, 75

Rodonò, M., Lanza, A. F., & Becciani, U. 2001, A&A, 371, 174

Rodonò, M., Messina, S., Lanza, A. F., Cutispoto, G., & Teriaca, L. 2000, A&A, 358, 624

Rucinski, S. M., & Vandenberg, D. A. 1986, PASP, 98, 669

Rüdiger, G., & Elstner, D. 1994, A&A, 281, 46

Saar, S. H., & Brandenburg, A. 1999, ApJ, 524, 295

Scargle, J. D. 1982, ApJ, 263, 835

Schrijver, C. J., & Zwaan, C. 1991, A&A, 251, 183

Schüssler, M., & Solanki, S. K. 1992, A&A, 264, L13

Schüssler, M., Caligari, P., Ferriz-Mas, A., Solanki, S. K., & Stix, M. 1996, A&A, 314, 503

Schwarzschild, M. 1975, ApJ, 195, 137

Spruit, H. C. 1982, A&A, 108, 348

Spruit, H. C., & Weiss, A. 1986, A&A, 166, 167

Tout, C. A., & Hall, D. S. 1991, MNRAS, 253, 9

Tunca, Z., İbanoğlu, C., Tumer, O., Ertan, A. Y., & Evren, S. 1983, Ap&SS, 93, 431

Umana, G., Trigilio, C., Hjellming, R. M., Catalano, S., & Rodonò, M. 1993, A&A, 267, 126

Vogt, S. S., Penrod, G. D., & Hatzes, A. P. 1987, ApJ, 321, 496